Universidade de Lisboa

Faculdade de Farmácia

INVESTIGATION OF LANA: A HUMAN VIRUS TUMOR GENE

Anita Marisa Pinto Sousa

Dissertation supervised by Professor João Pedro Monteiro e Louro Machado de Simas and co-supervised by Professor Maria João Carlos da Silva Gama.

Master's degree in Biopharmaceutical Sciences

2019

Universidade de Lisboa

Faculdade de Farmácia

INVESTIGATION OF LANA: A HUMAN VIRUS TUMOR GENE

Anita Marisa Pinto Sousa

Dissertation supervised by Professor João Pedro Monteiro e Louro Machado de Simas and co-supervised by Professor Maria João Carlos da Silva Gama.

Master's degree in Biopharmaceutical Sciences

2019

Resumo

Os herpesvírus pertencem à grande família de vírus, *Herpesviridae* e distinguem-se pela sua capacidade de infetar uma enorme variedade de hospedeiros. Até à data, foram identificados oito herpesvírus capazes de infetar humanos e estima-se que quase toda a população adulta esteja infetada por pelo menos um dos vírus pertencentes a esta família. Os os herpesvírus humanos são capazes de se adaptar ao meio intracelular do hospedeiro e escapar ao seu sistema imunitário estabelecendo uma infeção crónica que pode permanecer em estado de latência durante toda a vida do hospedeiro. No entanto, estes vírus normalmente não são causadores de doenças graves, a não ser que o sistema imunitário do hospedeiro esteja extremamente debilitado. A família *Herpesviridae* pode ser dividida em 3 subfamílias: alfa, beta e gama. E, tendo em conta os vírus capazes de infetar humanos, a família alfa inclui os herpesvirus simplex (HHV-1 e HHV-2) e o vírus varicela-zóster (HHV-3). Os herpesvírus pertencentes à subfamília beta são o citomegalovírus (HHV-5), HHV-6 (variantes A e B) e ainda o HHV-7. Finalmente, os membros da família gama são o vírus Epstein-Barr (HHV-4) e o herpesvírus associado ao sarcoma de Kaposi (HHV-8) e são associados a alguns tipos de doenças cancerígenas. Estes vírus são capazes de induzir a proliferação de células B infetadas através de reações que ocorrem no centro germinativo e expandir a latência viral às células B de memória, que são o maior reservatório de latência dos gamaherpesvírus. Em particular, o herpesvírus associado ao sarcoma de Kaposi (KSHV), um dos sete vírus causadores de cancro até hoje conhecidos, evoluiu no sentido de perturbar os mecanismos celulares normais do hospedeiro como o crescimento celular, a apoptose e até mesmo o sistema imunitário bem como as respostas antivirais. Esta contínua desregulação celular ao longo dos anos pode eventualmente levar ao desenvolvimento de doenças neoplásticas, principalmente em indivíduos imunocomprometidos. Sabe-se que o KSHV é o agente etiológico responsável pelo linfoma primário de efusão primário, pela doença de Castleman multicêntrica e pelo sarcoma de Kaposi, que é o tipo de cancro mais comum em pacientes infetados com o vírus da imunodeficiência humana (HIV).

O ciclo de vida do KSHV, tal como os outros herpesvírus, pode ser distinguido em duas fases distintas: uma fase lítica e uma fase de latência. Após a infeção inicial, os genes de ambas as fases são expressos mas após alguns ciclos de replicação viral, a fase lítica decresce e a fase de latência é estabelecida. Para que o genoma viral se mantenha nas células em divisão, o episssoma viral associa-se às histonas e estabelece-se como um cromossoma extra no núcleo

das células infetadas com expressão genética muito limitada. Esta reduzida expressão genética ajuda o vírus a escapar ao sistema imunitário do hospedeiro e ao mesmo tempo garante a sua sobrevivência e persistência viral. Uma das principais características deste tipo de vírus é sua capacidade de persistir no hospedeiro através da manutenção da latência viral, o que requer proteínas virais e celulares. Cerca de 90% das células infetadas possui o programa genético necessário à manutenção da latência viral. O programa de latência traduz-se num locus, onde são expressos vários genes que codificam para proteínas essenciais à latência viral, tal como a LANA (*Latency-associated Nuclear Antigen*).

A LANA é considerada a proteína responsável pela persistência viral e, consequentemente pela latência viral. É uma proteína multifuncional, sendo maioritariamente responsável pela segregação, replicação e manutenção do episssoma. No entanto, a LANA pode também interferir com os mecanismos de transcrição e interagir com diversas proteínas celulares e interferir com os mecanismos anti-tumorais do hospedeiro. A LANA, atuando como uma ubiquitina ligase E3, é capaz de regular a transcrição e sinalizar para degradação proteossomal supressores tumorais tais como o *von Hippel-Lindau* (VHL), o p53 ou ainda o *nuclear factor-kappa* B (NF-κB). A ubiquitinação está presente em todas as células eucarióticas e é um mecanismo regulatório essencial no ciclo celular, na apoptose, na endocitose ou ainda na resposta imunitária. Sendo assim, o KSHV, desenvolveu mecanismos com o objetivo de modular o seu funcionamento a seu favor. A ubiquitinação é um processo que ocorre através de uma cascata enzimática constituída por 3 enzimas: E1 (enzima ativadora da ubiquitina), E2 (enzima conjugadora) e E3 (ubiquitina ligase). Numa primeira etapa há a ligação da ubiquitina à E1 que, depois de ativada, é transferida para uma E2 que, juntamente com uma E3, transferem a ubiquitina para o substrato proteico para que seja degradado via proteossoma. A enzima E3 parece ser a responsável pelo reconhecimento específico do substrato e existem vários tipos de E3, tal como as Ellongin BC-Cullin5-SOCS (EC_5S). As EC_5S são complexos proteicos constituídos por várias subunidades, incluindo uma Cullin5 que se liga a uma Rbx1, formando assim o módulo Cullin 5-Rbx1, um heterodímero Elongin BC e uma proteína de reconhecimento de substrato SOCS (*supressor of cytokine signaling*). Todas as proteínas SOCS possuem uma homologia de sequência de 40 aminoácidos conservada – motivo SOCS-box. Este motivo SOCS-box é o responsável pela interação entre a Elongin BC e a Cullin5, estabelecendo a ligação entre o substrato de ubiquitinação e a E2. O complexo Elongin BC é um regulador positivo da RNA polimerase II e possui duas subunidades reguladoras (B e C). Este complexo desempenha um papel importante na regulação da transcrição e ainda ajuda a estabelecer a ligação entre as proteínas SOCS e as Cullin 5. Curiosamente, a proteína viral LANA possui uma SOCS-box

bipartida: BC-box + Cullin-box, localizadas na região C-terminal e N-terminal da proteína, respetivamente. Esta sequência proteica BC-box interage com uma Elongin C e estabelece um complexo proteico LANA-Elongin BC, que por sua vez ao ligar-se a um complexo Cullin5/Rbx reconstitui o complexo proteico: Ellongin BC-Cullin5-SOCS. Este complexo assemelha-se ao EC_5S, funcionando como uma ubiquitina ligase, modulando os mecanismos de ubiquitinação do hospedeiro a favor do vírus.

A infeção causada pelo KSHV é naturalmente limitada a humanos, por isso é muito importante o estabelecimento de um modelo animal de infeção para que o seu mecanismo de patogénese viral possa ser estudado *in vivo*. Visto que o herpesvirus murídeo 68 (MHV68), um vírus endémico que infeta o rato-do-campo Europeu e é capaz de infetar ratinhos de laboratório (*Mus musculus*), partilha alguma homologia de sequência genómica com o KSHV e codifica uma proteína homóloga à LANA do KSHV (mLANA), pode ser utilizado para a infeção de ratinhos de laboratório, providenciando um excelente modelo de estudo para o KSHV. A mLANA também possui uma região C-terminal, é expressa nas células B do centro germinativo e está envolvida na persistência do episssoma viral. Por último, a mLANA também é capaz de regular a transcrição genómica através de um complexo proteico EC_5S, que é mediado por uma "SOCS-box" viral que partilha alguma homologia com a SOCS-box presente na kLANA.

Neste projeto, tirando partido do modelo de infeção já estabelecido no laboratório, foram gerados vírus quimera (v-kLANA Elo-BC 46 e v-KM Elo-BC 34) com mutações na BC-box da kLANA (T212A, L213A, N214A, P215A, I216A, C217A) com o objetivo de avaliar a importância deste motivo na patogénese viral *in vivo*. O v-kLANA é um vírus quimera em que a mLANA foi substituída pela kLANA completa, incluindo a sua região 5´UTR e o v-KM é um vírus quimera que contém uma proteína de fusão entre a kLANA e a mLANA, ou seja, possui a kLANA mas com a região C-terminal da mLANA. Após mutagénese e reconstituição dos vírus quimera mutantes, 80 ratinhos foram divididos em 4 grupos distintos de infeção e inoculados com o vírus correspondente: 2 grupos com os vírus controlo (v-kLANA e v-KM) e 2 grupos com os vírus mutantes (v-kLANA Elo-BC 46 e v-KM Elo-BC 34). Aos dias 5, 7 e 10 pós infeção os ratinhos foram sacrificados e os pulmões foram devidamente extraídos e aos dias 10, 14 e 21 pós infeção os baços foram cirurgicamente removidos, *post mortem*. Após o processamento dos pulmões e baços, foi possível calcular os títulos virais na fase lítica e latente, respetivamente, e ainda averiguar o número de células positivas nos baços para DNA viral.

Os resultados demonstraram que as mutações inseridas na BC-box da kLANA não afetaram a expressão proteica e, no geral, também não afetaram a fase lítica do vírus nos pulmões. Estes resultados permitem concluir que os vírus mutantes v-kLANA Elo-BC 46 e v-KM

Elo-BC 34 são ambos viáveis. No entanto, os resultados *in vivo* não permitiram tirar conclusões acerca da importância e possível função da BC-box na latência, o que significa que estudos futuros terão de ser feitos no sentido de confirmar ou refutar os fenótipos virais descritos neste projeto.

Palavras chave: KSHV, LANA, latência, ubiquitinação, SOCS-box, BC-box, Cullin-box, EC5S ubiquitina ligase

Abstract

Kaposi's sarcoma-associated herpesvirus (KSHV) is one of the seven recognized human tumor viruses. It is the etiologic agent underlying Kaposi sarcoma, primary effusion lymphoma and multicentric Castleman's disease. This gammaherpesvirus establishes a lifelong persistence infection in the host and displays a lifecycle with two distinct phases: a short productive lytic phase and a prolonged latent phase. Latency-associated nuclear antigen (LANA) is the major latent gene and is strongly expressed in all forms of KSHV-associated malignancies. LANA mediates episomal replication, segregation and persistence, which is required for long-term maintenance of viral DNA. LANA proteins are also modulators of transcription through E3-ubiquitin ligase activity. Ubiquitination is an essential regulatory mechanism in eukaryotes, controlling a wide range of cellular pathways, including protein degradation. KSHV, like other viruses, has evolved mechanisms to hijack protein degradation pathways in order to establish an environment that favors its propagation. LANA protein has a bipartite SOCS-box motif divided into a Cullin-box and a BC-box located within its C-terminal and N-terminal regions, respectively. The BC-box interacts with an Elongin C and establishes a LANA-Elongin BC complex, which associates with a Cullin/Rbx1 module thus reconstituting a complex protein with E3 ubiquitin-ligase activity. This complex protein assembles an EC_5S ubiquitin ligase, which enables the virus to hijack the E3 ligase components of the cell, thus modulating the ubiquitination pathway of its host. In this project, by taking advantage of the MHV68 *in vivo* model to study KSHV pathogenesis, chimeric viruses with engineered mutations within the BC-box were generated in order to assess the importance of the BC-box motif within the kLANA N-terminal region. Results showed that mutations within kLANA BC-box neither affect protein expression or viral growth *in vivo* and viral lytic phase in the lungs was not significantly affected. Latency results were not conclusive and therefore the importance and role of kLANA BC-box is still unclear and viral phenotypes need to be reassessed.

Key words: KSHV, LANA, latency, ubiquitination, SOCS-box motif, BC-box, Cullin-box, EC5S ubiquitin ligase

Aknowledgements

Em primeiro lugar, agradeço ao Doutor Pedro Simas, por me ter dado a oportunidade de desenvolver a minha tese de mestrado no seu laboratório, por ter partilhado o seu vasto conhecimento científico comigo e pela disponibilidade, atenção e simpatia que sempre demonstrou ao longo deste ano. Gostaria também de agradecer à Doutora Marta Miranda, por todo o acompanhamento científico e conselhos dados durante o meu percurso no laboratório, foram sem dúvida indispensáveis para atingir os meus objetivos.

Queria agradecer à Doutora Cecília Rodrigues, a coordenadora do Mestrado em Ciências Biofarmacêuticas e à Doutora Maria João Gama, a minha orientadora interna, pela disponibilidade e simpatia que sempre demonstraram para esclarecer todas as minhas dúvidas.

Agradeço à Doutora Andreia Mósca, por toda a orientação científica, paciência e calma (muita calma), mesmo nos momentos mais difíceis e, acima de tudo, pela amizade.

Gostaria de agradecer à minha colega de laboratório, Catarina Costa, que conheci no início deste ano letivo, mas que com certeza levarei comigo por muitos mais anos. Obrigada pelo apoio incondicional, pela ansiedade e pânico partilhados, pelos serões no iMM, pelas gargalhadas até doer a barriga e por teres sido a minha pessoa no laboratório durante este ano.

Queria agradecer à minha amiga, Catarina Ferreira, que esteve comigo desde o início desta longa e difícil jornada que é a vida académica. Obrigada pelo companheirismo, pela cumplicidade, amizade, carinho e compreensão. Sei que, mesmo quando estamos juntas no mesmo barco (estamos sempre, infelizmente) de uma coisa posso ter a certeza, no meio do pânico e do caos, é sempre melhor estar contigo. Obrigada Cacá por estares sempre presente nos bons e maus momentos, és uma amiga incansável e com quem sei que poderei sempre contar.

Obrigada ao Filipe Rodrigues, o meu melhor amigo e o meu “partner in crime”. Agradeço-te por me teres ouvido sempre que precisei, por me ter queixado (quase) sem parar ao longo deste ano e por, mesmo assim, não te teres fartado e teres sempre dito que ia tudo correr bem e que acreditas em mim. Obrigada por estares presente na minha vida, por sentires quando é que preciso de uma ida ao café, de um jantar, de dançar ou simplesmente de uma chamada telefónica para me animar, obrigada por seres tu.

Um obrigada muito especial à minha irmã, Priscila Sousa Gonçalves, que é também a minha melhor amiga e a melhor conselheira do mundo. Agradeço-te por todo o teu apoio incondicional, por me protegeres desde que nasci, por todos os miminhos, abraços, carinhos, almoços, jantares e festas. Obrigada pelas nossas conversas infinitas, por conheceres e perceberes cada particularidade minha e por partilhares esta personalidade peculiar comigo (assim não me sinto sozinha no mundo). Queria agradecer também ao teu marido, Élvio Sousa Gonçalves, que muito tem aturado ao longo destes 15 anos e que é como um irmão para mim.

À minha mãe, Ana Sousa, que é a melhor pessoa que eu conheço e o melhor exemplo feminino que poderia ter. Obrigada por seres o pilar da família Sousa: és a nossa calma na tempestade, o quentinho no Inverno e o sol no Verão. Obrigada por me ouvires, mesmo não percebendo tudo, e por me apoiares incondicionalmente. És a minha "personal cheerleader" e melhoras a minha vida todos os dias, obrigada mami. Ao meu pai, Francisco Sousa, que é o maior sonhador que eu alguma vez conheci. Ensinou-me que podemos e devemos ter muitos sonhos e que não faz mal que nem todos se concretizem, basta apenas alguns. E, nem sempre os sonhos se realizam exatamente da forma que idealizámos, mas não faz mal, às vezes são ainda melhores. Ensinou-me também, através da sua garra, luta, perseverança e inteligência que podemos alcançar aquilo que planeamos para nós e que "nunca se sabe onde é que estaremos daqui a 10 anos" (é um otimista no fundo). Obrigada por teres sido, muitas vezes, o impulsionador de alguns sonhos e aventuras minhas e por todo o apoio subentendido nas tuas palavras e ações. Com a vossa ajuda consegui encerrar mais um capítulo da minha vida. Obrigada.

Finalmente, queria agradecer ao meu namorado, Joaquim Torres, que é o melhor companheiro de aventuras que alguma vez tive. Obrigada por teres sido incansável ao longo deste ano e por me fazeres rir a toda a hora. Dizem que "rir é o melhor remédio" e não podia estar mais de acordo. Não és da minha área, mas durante este ano ouviste-me a toda a hora, todos os dias e tentaste aconselhar-me da melhor forma, mesmo quando tu próprio tiveste dias menos bons. Obrigada por acreditares em mim mais do que eu própria (às vezes) e por me fazeres sentir que, contigo na minha vida, vai sempre correr tudo bem.

Table of contents

Chapter 1: Introduction 16
1. Cancer virology 16
2. Herpesviridae family 17
2.1 Gammaherpesvirus subfamily: Kaposi's sarcoma-associated herpesvirus 18
2.1.1 Clinical diseases associated with KSHV infection 19
2.1.2 KSHV infection and the host immune response 20
2.1.3 KSHV viral lifecycle 22
2.1.4 The KSHV latency-associated nuclear antigen 23
2.1.5 LANA and its role during ubiquitination 25
2.2 MHV68: a KSHV study model 26
2.2.1 Chimeric virus – v-kLANA 28
2.2.2 Chimeric virus – v-KM 28
Significance 29
Chapter 2: Materials and Methods 30
1. Generation of MHV-68 recombinant viruses 30
1.1 Plasmids 30
1.2 DNA: isolation and analysis 31
1.2.1 Plasmid DNA purification 31
1.2.2 Quantification and sequencing of DNA 32
1.2.3 Restriction endonuclease reactions 32
1.2.4 DNA ligation 32
1.2.5 Analysis and isolation of DNA by gel electrophoresis 33
1.3 Bacterial strains 33
1.3.1 Super Competent E.coli cells preparation 33
1.3.2 Transformation of competent cells 34
1.4 Cloning procedures to engineer v-kLANA Elo-BC and v-swap Elo-BC viruses 34
1.4.1 Mutagenesis: Polymerase Chain Reaction (PCR) to introduce mutations into pSP72_PCR1_PCR3 34
1.4.2 Subcloning the pSP72_PCR1_3 Elo-BC into pSP72_PCR1_5 and pSP72_994swap 36
1.4.3 Subcloning pSP72_swap Elo-BC and pSP72_PCR1_5 Elo-BC into BamHI-shuttle vector 36
1.5 BAC mutagenesis 36

1.5.1 BAC DNA preps 38
1.6 Cell lines 39
1.7 Viruses 39
1.8 Reconstitution of MHV-68 viruses 40
1.8.1 Virus reconstitution on BHK-21 cells 40
1.8.2 Passage through NIH3T3-Cre cells to remove BAC sequences 41
1.9 Production of viral stocks: working stock media (WSM) and cell working stock (CWS) 41
1.10 Virus titration using the suspension method: plaque assay 41
2. Protein expression analysis 42
2.1 Sodium dodecyl sulfate-polyacrylamide gel electrophoresis (SDS-PAGE) 42
2.2 Transference of proteins into nitrocellulose membranes 43
2.3 Western blot 43
3. Ethics statement 44
4. Mice 44
5. In vivo assays 44
5.1 Infection of mice 44
5.2 Lung viral titration 45
5.3 Single cell suspensions 45
5.4 Infectious Center Assay (ex vivo explant co-culture assay) 46
5.5 Limiting dilution assay and real-time PCR of viral DNA positive cells 46
6. Statistical analysis 47
Chapter 4: Results and Discussion 47
1. Generation and characterization of MHV68 recombinant virus 47
2. In vitro assays 50
2.3 Viral titration 50
2.4 Expression of kLANA mutant proteins 51
3. In vivo assays 52
3.1 Lung viral titres 52
3.2 Infectious center assay and quantification of viral DNA-positive total splenocytes 53
Chapter 5: Conclusion and future perspectives 56
References 58
Supplementary data 63

Table index

Table 1 - Human herpesviruses classification 18
Table 2 - Primers used for sequencing 32
Table 3 - Primers used in the mutagenesis strategy 36
Table 4 - Primers used in the colony PCR 38
Table 5 - List of MHV68 recombinant virus constructed during this project 40
Table 6 - Antibodies used in the western blot assay 43
Table 7 - *in vivo* experiments 45
Table 8 - Viral stock titers 51
Table 9 - Reciprocal frequency of viral DNA positive cells in total splenocytes 56

Figure index

Figure 1 - Episome segregation model....24
Figure 2 - A model for KSHV LANA assembles EC_5S ubiquitin complex to target downstream substrates for degradation....26
Figure 3 - Schematic representation of LANA and ORF73. Proteins with the putative SOCS-box motifs indicated....27
Figure 4 - Representation of kLANA proteins expressed by each virus, highlighting the kLANA SOCS-box motif....48
Figure 5 - Restriction profiles of non-yfp BAC plasmids and schematic representation of MHV68 genome with each restriction enzyme sites....50
Figure 6 - BAC cassette removal through NHI-3T3 cells expressing Cre recombinase....50
Figure 7 - Expression detection of viral protein kLANA....51
Figure 8 - Lung viral titration. BALB/cByJ mice were intranasally inoculated with 10^4 PFU....52
Figure 9 - Assessment of latent infection in the spleens of infected mice....54
Figure 10 - Subcloning the pSP72_PCR1_3 Elo-BC into pSP72_PCR1_5 (A) and pSP72_994swap (B)....63
Figure 11 - Subcloning pSP72_PCR1_5 (A) and Elo-BC pSP72_swap Elo-BC (B) into BamHI-shuttle vector....64
Figure 12 - BAC mutagenesis strategy....64
Figure 13 - Passage through NIH3T3-Cre cells to remove BAC sequences....64

Abbreviations

AmpR: Ampicilin resistance

BAC: Bacterial artificial chromosome

BHK: Baby hamster kidney

CMV: Cytomegalovirus

CRL: Cullin RING ligase

CPE: Cytopathic effect

CWS: Cell working stock

DBD: DNA binding domain

DMEM: Dulbecco's modified Eagle medium

DPI: Days post-infection

dsDNA: Double-stranded DNA

EBV:Epstein-Barr virus

EC_5S: ElonginBC-Cullin5-SOCS

EQE: Glutamate- and glutamine-rich region

FBS: Fetal bovine serum

GC: Germinal center

GFP: Green fluorescent protein

HAART: highly active antiretroviral therapy

HBV: Hepatitis B virus

HCV: Hepatitis C virus

HHV-1 to 8: Human herpesvirus 1 to 8

HIFα: Hypoxia-inducible factor 1-alpha

HIV: Human immunodeficiency virus

HPV: Human papillomaviruses

HSV: Herpes simplex virus

HTLV-1: Human T-lymphotropic virus-I

HUVECs: Human endothelial cells

IARC: Internation Agency for Research on Cacer

ICA: Infectious center assay

IE: Immediate early

IFN: Interferon

IRFs: Interferon regulatory factors

KanR: Kanamycin resistance

KS: Kaposi's sarcoma

KSHV: Kaposi's sarcoma-associated virus

LANA: Latency-associated nuclear antigen

LB: Luria-Bertani

LBS: LANA binding sites

MCD: Multicentric Castleman's disease

MHV68: Murine gammaherpesvirus 68

miRNA: micro RNA

MOI: Multiplicity of infection

NF-κB: Nuclear factor kappa B

NLRs: NOD-like receptors

O/N: Overnight

ORF: Open reading frame

PAMPs: Pathogen-associated molecular patterns

PCR: Polymerase chain reaction

PEL: Primary effusion lymphoma

PFU: Plaque forming unit

PRRs: Pattern recognition receptors

RBL: Red blood lysis buffer

RLRs: Retinoic acid-like receptors

RT: Room temperature

RTA: Replication and transcription activator

SOCS: Suppressor of cytokine signaling protein

ssDNA: Single-stranded DNA

TERT: telomerase reverse transcriptase

TGFβ: Transforming growth factor beta

TLRs: Toll-like receptors

TPA: 12-O-tetradecanoyphorbol-13-acetate

TR: Terminal repeats

UTR: Untranslated region

VHL: von Hippel-Lindau

vIRFs: Viral interferon regulatory factors

VZV: Varicella-zoster virus

WB: Western blot

WSM: Working stock media

WT: Wild type

YFP: Yellow fluorescent protein

Chapter 1: Introduction

1. Cancer virology

It is widely accepted that viruses play a significant role in the development of particular cancers in many different animals, including humans (Cooper, 1995). Indeed, according to the International Agency for Research on Cancer (IARC) approximately 12% to 20% of human cancers are caused by viruses. Viruses have been key elements to modern cancer research and provide profound insights into possible different cancer causes, whether they are infectious or non-infectious (Moore and Chang, 2010). The first described human tumor virus was the Epstein-Barr virus (EBV) in 1964 and, until now, six more human cancers have been described: Hepatitis B virus (HBV) (1965), Human T-lymphotropic virus-I (HTLV-I) (1980), High-risk human papillomaviruses (HPV) (1983-1984), Hepatitis C virus (HCV) (1989), Kaposi's sarcoma-associated herpesvirus (KSHV) (1994) and finally Merkel cell polymarirus (MCV), in 2008 (Moore and Chang, 2010). However, there is no obvious molecular rule able to firmly establish or eliminate an agent as a potential human tumor virus *a priori*, and almost all of the tumor viruses have very close relatives that do not cause cancer in humans (Moore and Chang, 2010). Thus, why do some viruses actually cause cancer? Since tumors do not increase the virus transmissibility or its fitness, one possible explanation is that cancers caused by viruses are biological accidents. Moreover, tumors are "dead-ends" for viruses and only a few people infected with any of the existing tumor viruses eventually develop cancer.

Viruses can cause cancer by interacting with host proteins, proliferating when the host immune system is weakened, and hijacking proliferating host cells (Wen and Damania, 2010). Compared to other viruses, human tumor viruses are unusual because they infect, but do not kill, their host cells. This allows human tumor viruses to establish persistent chronic inflammation leading to tissue damage, which is one of the known mechanisms of carcinogenesis (Goossens and Hoshida, 2015). Moreover, tumor viruses are strongly selected to encode oncogenes able to initiate tumorigenesis, such as oncoproteins that target p53, telomerase reverse transcriptase (TERT), cytoplasmic PI3K/AKT/mTOR, nuclear factor-κB (NF-κB), β-catenin or interferon signaling pathways (Mesri, Cesarman and Boshoff, 2010; Moore and Chang, 2010; Dissinger and Damania, 2016; Dittmer *et al.*, 2016). It is thought that these viral oncogenes target cellular tumor suppressor pathways to re-initiate the cell cycle entry of differentiated cells to promote viral replication. The result is cellular genomic instability and aneuploidy, which contributes to carcinogenesis (Moore and Chang, 2010). The other theory is based on large DNA tumor viruses, such as EBV or KSHV. This theory suggests a more complex interaction between viral oncogenes

and host, where the virus main goal is to evade immune responses during the latency program rather than assuring viral genome replication (Moore and Chang, 2003, 2010).

Despite the already recognized importance of tumor causing viruses by the scientific community, there is still a considerable amount of work to do in this research area. For instance, EBV has been discovered 55 years ago and there is still no vaccine. Moreover, KSHV has emerged as a leading cause of adult cancer in sub-Saharan Africa and the Kaposi sarcoma (KS) is the most common cancer in individuals living with HIV nowadays (Schulz and Cesarman, 2015). Although no movement has yet been made for the pursuit of clinical interventions. Thus, the development of anti-latent viral strategies and immunological therapies against these cancer viruses is critical.

2. Herpesviridae family

Human herpesviruses have large (100-200 nm) and double stranded DNA (ds-DNA) genomes enclosed inside the viral protein cage (capsid), surrounded by a tegument layer which is enclosed in a lipid envelope constituted with glycoproteins (Chakraborty, Veettil and Chandran, 2012; Grinde, 2013). The family name *Herpesviridae* is derived from the Greek word *herpein* meaning "to creep", which refers to the latent, recurring infections, typical of this family of viruses. All human herpesviruses are able to adapt very well to the cellular milieu of the host and evade his immune system, establishing life-long latent infection (Wen and Damania, 2010). Considering gene diversity, herpesviruses are among the most complex human viruses due to the 70-200 open reading frames (ORFs) of their genomes (Grinde, 2013). This large repertoire of herpes genes allows a persistent infection in the host through cell manipulation and immune evasion.

Up to date, there are eight known herpesviruses that commonly infect humans and approximately all of the adult population is infected with at least one of these (Grinde, 2013). Although, these viruses are highly unlikely to cause severe disease, unless the host immune system is already compromised. The Herpesviridae family can be classified into 3 different subfamilies, according to their host range, replication cycle and cell tropism: alpha, beta and gamma (Roizman B, Carmichael LE, Deinhardt F, de-The G, Nahmias AJ, Plowright W, Rapp F, Sheldrick P, Takahashi M, 1981). The human alpha subfamily includes herpes simplex viruses (HHV-1 and HHV-2) and varicella-zoster virus (HHV-3). Human herpesviruses belonging to the betaherpesvirinae subfamily are cytomegalovirus (HHV-5), HHV-6 variants A and B and HHV-7. Finally, the members of the gamma subfamily are strongly associated with neoplastic diseases:

Epstein-Barr virus (HHV-4) and Kaposi's sarcoma-associated herpesvirus (HHV-8) (Boshoff and Chang, 2001; Wen and Damania, 2010).

Table 1 - Human herpesviruses classification

Formal name	Trivial name (acronym)	Subfamily	Primary targets	Main sites of latency
Human herpes virus 1	Herpes simplex virus-1 (HSV-1)	Alpha	Mucoepithelia	Sensory and cranial nerve ganglia
Human herpes virus 2	Herpes simplex virus-2 (HSV-2)	Alpha	Mucoepithelia	Sensory and cranial nerve ganglia
Human herpes virus 3	Varicella zoster virus (VZV)	Alpha	Mucoepithelia	Sensory and cranial nerve ganglia
Human herpes virus 4	Epstein-Barr virus (EBV)	Gamma	Epithelial and B cells	Memory B-cells
Human herpes virus 5	Cytomegalovirus (CMV)	Beta	Monocytes, lymphocites and epithelial cells	Monocytes and lymphocites
Human herpes virus 6A and 6B	Roseola virus (HHV-6)	Beta	T-cells	Leukocytes
Human herpes virus 7	Roseola virus (HHV-7)	Beta	T-cells	T-cells and epithelia
Human herpes virus 8	Kaposi's sarcoma-associated herpesvirus (HHV-8)	Gamma	Epithelial and endotelial cells	B-cells and monocytes

2.1 Gammaherpesvirus subfamily: Kaposi's sarcoma-associated herpesvirus

The gammaherpesviruses persistent infection is highly associated with several human malignancies, including some types of tumors (Dirk P. Dittmer, 2013). These viruses are able to induce proliferation of latently infected B cells through reactions that occur in the germinal center (GC), expanding latency and gaining access to memory B cells, the major reservoir of gammaherpesviruses latency (Cerqueira *et al.*, 2016).

Kaposi's sarcoma-associated herpesvirus, also known as herpesvirus 8 (HHV-8), is one of the seven recognized human cancer-causing viruses that has evolved to subvert the normal cellular pathways of its host through a plethora of viral gene products (Moore and Chang, 2010). The KSHV genome consists of ~165 kb, encompassing the several KSHV ORFs, flanked by 30-kb terminal repeat (TR) sequences (Juillard *et al.*, 2016; Purushothaman *et al.*, 2016).

Upon infection, the linear KSHV genome is transported to the nucleus, circularizes and is maintained as an episome (Purushothaman *et al.*, 2016). This gammaherpesvirus is able to

dysregulate the cell cycle progression, apoptosis, immune surveillance and even antiviral responses of the host (Dittmer *et al.*, 2016). This disturbance contributes to host cell transformation and eventually to the development of neoplastic disorders, most frequently in immunodeficient individuals (Wen and Damania, 2010). Although the International Agency for Research on Cancer classified KSHV as a class I carcinogen, the majority of KSHV infections have no immediate clinical symptoms and, as with other human neoplastic viruses, cancer only emerges decades after infection (Thakker and Verma, 2016).

2.1.1 Clinical diseases associated with KSHV infection

KSHV is the etiologic agent underlying primary effusion lymphoma (PEL), multicentric Castleman's disease (MCD) and Kaposi's sarcoma (KS), the leading AIDS malignancy (Schulz and Cesarman, 2015).

Kaposi's sarcoma

In 1872, the Austrian-Hungarian dermatologist Moritz Kaposi described five cases of a lethal and previously unknown "idiopathic multiple pigmented sarcomas of the skin". This form of disease was designated Kaposi's sarcoma only in 1891 (Boshoff and Chang, 2001). In 1994, hespesvirus-like DNA sequences were identified in KS tissue through analysis of DNA fragments obtained from KS biopsies (Chang *et al.*, 1994). This newly identified virus was then named Kaposi's sarcoma-associated herpesvirus (KSHV) or human herpesvirus-8 (HHV-8), the eighth member of the *Herpesviridae* family. KS can be classified into 4 distinct clinical subtypes, based on the epidemiological and clinical outcomes: classic/sporadic, endemic/African, epidemic/AIDS-associated, and iatrogenic/post-transplant (Wen and Damania, 2010). Classic KS, the tumor first described by Kaposi, affects mainly elderly males of Mediterranean or eastern European origin (Gramolelli and Schulz, 2015). Endemic KS is clinically more aggressive, with more lymph node involvement than classic KS, and is commonly seen in children of sub-Saharan Africa and is associated with high mortality rates (Wen and Damania, 2010; Dirk P. Dittmer, 2013). AIDS-associated KS, is the most clinically aggressive variant found in patients, however through highly active antiretroviral therapy (HARRT) and the resulting immune reconstitution, the incidence and mortality of AIDS-associated KS have dramatically dropped (Wen and Damania, 2010). Finally, the iatrogenic KS, develops in solid organ transplant recipients, because it is associated with immunosuppressive therapy after organ transplant (Dirk P. Dittmer, 2013). Renal transplant patients are the most likely group to develop this form of KS and usually, iatrogenic KS regresses

upon reduction or withdrawal of immunosuppressive therapy (Wen and Damania, 2010; Gramolelli and Schulz, 2015).

Primary effusion lymphoma

The primary effusion lymphoma (PEL) is a diffuse large B cell lymphoma of post germinal center origin (Dittmer *et al.*, 2016). Different from KS, PEL presents as a lymphomatous effusion tumor contained in various body cavities such as the pericardium, pleuron, and the peritoneum. PEL is a very aggressive tumor with rapid progress and a very poor prognosis associated with high mortality rates and a median survival time of two to six months (Wen and Damania, 2010). Cells with PEL contain many KSHV episomes (50 to 150 viral copies per cell) and they can either be KSHV single-positive or KSHV/EBV double positive (Wen and Damania, 2010; Dittmer *et al.*, 2016).

Multicentric Castleman's disease

Multicentric Castleman's disease (MCD) is a lymphoproliferative disorder, affecting multiple sets of lymph nodes and other tissues throughout the body (Dittmer *et al.*, 2016). MCD has two known variants: plasmablastic, which is highly associated with KSHV, and hyaline, which is not (Wen and Damania, 2010). In MCD caused by KSHV, there is a cytokine over activity caused by viral products, leading to atypical lymphoproliferations and potential progression to lymphoma. Plasmablastic MCD can be very aggressive and rapidly progress, thus causing high fatality (Wen and Damania, 2010). KSHV genomes, similar to KS and PEL patients, are detectable in almost all HIV-positive MCD cases and in about 50% of HIV-negative MCD cases (Moore and Chang, 2010).

2.1.2 KSHV infection and the host immune response

The human immune system works like a shield, designed and equipped to suppress a variety of diseases and yet, can never eliminate the Kaposi's sarcoma-associated herpesvirus. This is due to the fact that KSHV, like all the other members of his family, is able to establish lifelong infection in the host and evade viral clearance (Wen and Damania, 2010).

KSHV is thought to enter cells predominantly through the endocytic pathway, which involves envelope glycoproteins that mediate virus attachment, entry, assembly, and exit of virus (Chakraborty, Veettil and Chandran, 2012). Upon infection, KSHV leads to changes in cell morphology, glucose metabolism, growth rate, lifespan and gene expression (Mesri, Cesarman

and Boshoff, 2010). This gammaherpesvirus encodes approximately 86 ORFs, including several potential immunomodulators (K3, k5, K9, K11.1), and anti-apoptotic protein (K7) which regulates cytokine secretion, antagonizes host interferon (IFN)-mediated antiviral responses, and regulates immune evasion (Purushothaman *et al.*, 2016). KSHV is capable of infecting different cell types, hence possesses multiple viral receptors to enter the host cell (Dittmer *et al.*, 2016). During KSHV entry into the host cells, it encounters several innate immune patrol cells that trigger an antiviral response. Remarkably, it is likely that this innate immune response activation, during primary infection, induces the viral latent phase (Akula *et al.*, 2002; Wang *et al.*, 2003; Rappocciolo *et al.*, 2006).

The innate immune response is triggered through pattern recognition receptors (PRRs) that are able to recognize pathogen-associated molecular patterns (PAMPs). These PRRs are unique, meaning that each cell type expresses its own, and lead to the production of interferon and pro-inflammatory cytokines (Dittmer *et al.*, 2016). Thus, there is a multitude of PRRs in human cells including toll-like receptors (TLRs), retinoic acid-like receptors (RLRs) and NOD-like receptors (NLRs) (Dittmer *et al.*, 2016; Ma and Damania, 2016). During primary KSHV infection, activation of the different TLRs in monocytes results in interferon production and upregulation of both cytokines and chemokines (West and Damania, 2008; West *et al.*, 2011). Following *de novo* infection with KSHV and during viral reactivation, the cytosolic RIG-I-like receptor induces IFN-β production and suppresses viral gene expression (Inn *et al.*, 2011). As the members of the NLR family can sense PAMPs, they form inflammasomes which leads to cleavage and production of IL-1β and IL-18, two well-known pro-inflammatory cytokines (Jacobs and Damania, 2012).

Studies suggest a very thin and delicate equilibrium between viral infection and host response. Although the innate immune system activation induces KSHV into a latent state, a high degree of innate response also facilitates killing of the infected cells and tries to prevent latency. Thus, KSHV encodes several genes to escape the innate immune signaling pathways, which include viral interferon regulatory factors (vIRFs), complement regulatory proteins, tegument proteins and DNA-binding proteins (Dittmer *et al.*, 2016). KSHV encodes four different vIRFs, some ablate cellular IRF signaling and others inhibit IFN production (Jacobs and Damania, 2011). All herpesviruses encode for tegument proteins, which are early deposited into the cytoplasm following virion fusion and capsid release. ORF45 and ORF64 are tegument proteins that are able to block IRF7 phosphorylation and activation of type I IFN responses and encode potent deubiquitinating activity, respectively (Inn *et al.*, 2011; Dittmer *et al.*, 2016). ORF50 is a DNA-binding protein and a transcription factor, although it can also induce the degradation of innate immune responders such as IRF7 or TLR3. Lastly, latency-associated nuclear antigen (LANA) is

another DNA-binding protein that also inhibits IFN-β induction, through binding to its promotor, and the transcription of IFN-gamma-inducible genes (Cloutier and Flamand, 2010; Dittmer *et al.*, 2016). The adaptive immune system also plays an important role during KSHV infection. This herpesvirus expresses proteins that can affect either the antigen presentation, the B cell targeting, the MHC class I display, and even the neutrophil and basophil activation (Dittmer *et al.*, 2016).

2.1.3 KSHV viral lifecycle

Like other herpesviruses, KSHV comprehends two different lifecycle phases: latent and lytic. Following primary infection, the genes from both phases are expressed, but after some rounds of viral replication, the lytic gene expression decreases, and latency is established. Although, both lytic and latent cycle replications are important for the long-term maintenance of the virus in the host, and the gene products from both expression programs have critical roles in the pathogenesis of KSHV-associated diseases (Purushothaman *et al.*, 2016)(Fig.1).

KSHV viral episome associates with cellular histones and exists as an extra-chromosome in the nucleus of infected cells with the expression of limited viral genes. This allow the virus to maintain the genome in dividing cells and to escape the host immune responses while, at the same time, enhancing cell survival and virus persistence (Purushothaman *et al.*, 2016). A key feature of all herpesviruses infection is their lifelong persistence in the host by maintaining viral latency, which requires not only viral but also cellular proteins (Correia *et al.*, 2013; Dissinger and Damania, 2016). The latent transcriptional program is carried out in more than 90% of infected cells and has led to the characterization of a latency locus that is abundantly and consistently transcribed in all the KSHV infected cells. This latency locus contains several latency associated proteins such as vCyclin, vFLIP, miRNAs and LANA (Purushothaman *et al.*, 2016). Furthermore, to maintain latency, it is crucial that only latent genes are expressed while lytic gene transcription is repressed (Prasad *et al.*, 2012). In fact, studies have demonstrated that in actively transcribed latency regions, the chromatin presents an open configuration, lacks nucleosomes, and exhibits active histone marks, while lytic genes are present in the condensed chromatin regions (Toth *et al.*, 2010; Dissinger and Damania, 2016). This indicates that epigenetics plays a crucial role in the maintenance of latency through the interaction of histone modifiers and chromatin, and several other proteins such as LANA (Hu *et al.*, 2014). Latent KSHV expresses a very small subset of proteins in the infected cells, and no functional or infectious viral particles are produced.

The lytic cycle replication is characterized by the expression of linear viral genomes, and can be divided into three different phases: immediate early (IE), early, and late gene expression (Sun *et al.*, 1999). This process follows a highly orchestrated temporal order. The transcription of

IE genes does not require prior protein synthesis and are crucial for regulating the subsequent transcriptional cascade (Wen and Damania, 2010). Early gene expression requires proteins encoded by IE genes and late genes expression follows DNA replication. Late genes encode for structural proteins necessary for the envelope glycoproteins and also for the assembly of new virions (Dissinger and Damania, 2016). The lytic viral lifecycle is crucial for viral propagation and tumorigenesis through replication and constant infection of new cells (Aneja and Yuan, 2017).

The latent phase can be induced into the lytic phase with the addition of chemicals that activate the expression of IE genes and transcription activator (RTA), encoded by ORF50, which is the master regulator of KSHV lytic replication (Krishnan *et al.*, 2004). Those chemicals include 12-O-tetradecanoyphorbol-13-acetate (TPA) and sodium butyrate (Aneja and Yuan, 2017). These agents acting as extracellular stimuli, can also affect chromatin regulatory factors and as a result, the viral episome gradually relaxes from its compact chromatin structure, leading to the expression of all viral genes and the production of infectious virion particles from the lytic replication phase (Purushothaman *et al.*, 2016). However, the majority of infected cells bear the virus in the latent phase, and only 3-5% of the cells exhibit the productive lytic infection phase (Chudasama *et al.*, 2015). It is the balance between KSHV latent and lytic viral life cycles that enables the virus to escape immune surveillance and maintain persistent infection and propagate in the individual and maybe even spread to other individuals (Aneja and Yuan, 2017).

2.1.4 The KSHV latency-associated nuclear antigen

KSHV latency-associated nuclear antigen is a 1162 amino acid protein encoded by ORF73 of the viral genome (Juillard *et al.*, 2016). It is considered the viral protein responsible for viral persistence and the major gene of the latent viral lifecycle (Correia *et al.*, 2013; Purushothaman *et al.*, 2016). LANA mediates episomal replication, segregation and persistence, which is required for long-term maintenance of viral DNA into the daughter cells during mitosis (Correia *et al.*, 2013). The C-terminal region of kLANA harbors a DNA-binding domain (DBD) that self-associates and cooperatively binds to two adjacent sites in each terminal repeat (TR) DNA sequences of the viral episome, LANA-binding sites (LBSs) 1 and 2 (LBS1, LBS2) (Juillard *et al.*, 2016). LBS1 is a high affinity site which helps the binding of LANA to LBS2 and both sites contribute to LANA's ability to suppress transcription and facilitate DNA replication (Garber, Hu and Renne, 2002; Correia *et al.*, 2013). N-terminal kLANA region binds histones H2A and H2B on the nucleosome surface to attach to mitotic chromosomes (Barbera *et al.*, 2006; Juillard *et al.*, 2016). These binding properties together, allow LANA to form a molecular tethering apparatus

which ensures that viral genomes are segregated to daughter cell nuclei following mitosis (Correia *et al.*, 2013; Habison *et al.*, 2017) (Fig.1).

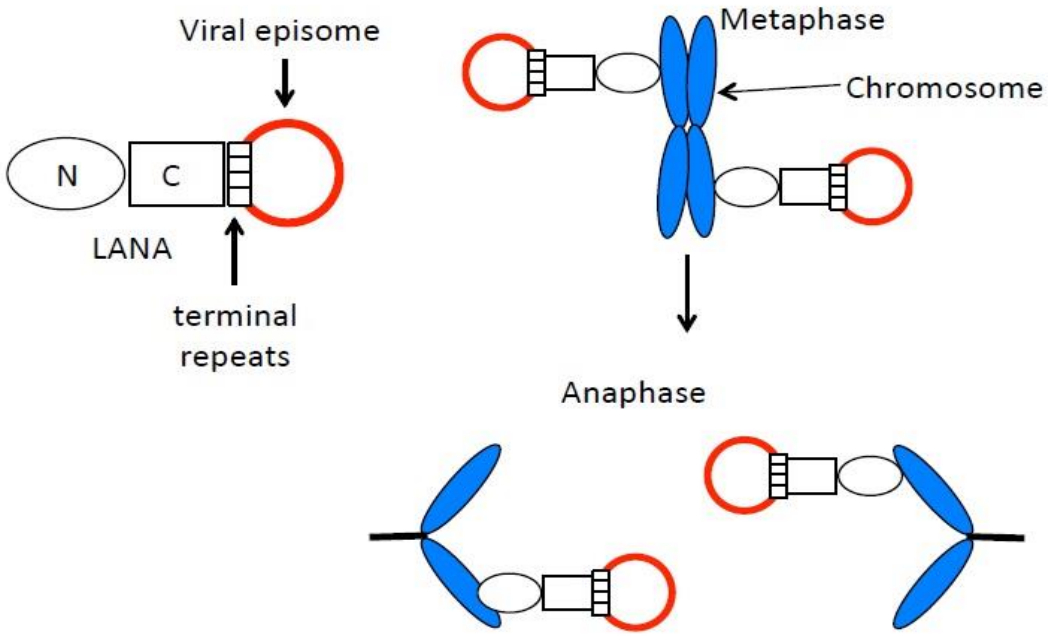

Figure 1 - Episome segregation model. C-terminal LANA (C) binds terminal repeat DNA sequences in the episome. N-terminal (N) associates with the nucleosome. These binding characteristics allow tethering of the episome to chromosomes during mitosis and segregation of episomes to daughter cells in anaphase.

Although the main function of LANA is to maintain the viral episome, this is a multifunctional nuclear protein that can also interfere with important anti-tumorigenic pathways (Si and Robertson, 2006; Mesri, Cesarman and Boshoff, 2010). Moreover, LANA has been shown to dysregulate Wnt signaling, through stabilization of β-catenin, and to inhibit anti-proliferative transforming growth factor-β (TGFβ 1), by epigenetic suppression of TGFβ receptors (Fujimuro *et al.*, 2003; Di Bartolo *et al.*, 2008). Indeed, LANA might also contribute to angiogenesis, a crucial step during the oncogenesis process, by stabilizing hypoxia-inducible factor 1α (HIF1α) (Cai *et al.*, 2006). LANA was also shown to upregulate the human telomerase reverse transcriptase (hTERT) gene expression and increase the lifespan of primary human umbilical vascular endothelial cells (HUVECs) (Watanabe *et al.*, 2003). This nuclear antigen, is also able to interfere with transcription and interact with several cellular proteins to modulate host functions involved in latency regulation and oncogenesis (Rodrigues *et al.*, 2009). Moreover, LANA is able to stabilize Myc, establishing a link between virus induced lymphoproliferation and disease (Rodrigues *et al.*, 2013). Finally, LANA is able to regulate transcription through E3-ubiquitin ligase activity (Correia *et al.*, 2013). LANA functions as a component of an ubiquitin complex that targets tumor

suppressors such as the von Hippel-Lindau (VHL), p53 and nuclear factor-kappa B (NF-κB) for degradation (Cai *et al.*, 2006; Rodrigues *et al.*, 2009).

2.1.5 LANA and its role during ubiquitination

Ubiquitination is an essential regulatory mechanism and is involved in nearly all aspects of eukaryotic biology such as signal transduction, development, apoptosis, cell cycle progression, endocytosis and even immune response (Cai *et al.*, 2006). Thus, KSHV, like other viruses, has developed mechanisms to modulate ubiquitination in its favor (Correia *et al.*, 2013). The ubiquitination process can be divided into two steps: (1) the covalent attachment of multiple ubiquitin molecules to the protein substrate and (2) the degradation of the ubiquitylated protein by the 26S proteasome complex (Cai *et al.*, 2006). This process occurs through a three-enzyme cascade involving E1 ubiquitin-activating enzyme, an E2 ubiquitin-conjugating enzyme, and an E3 ubiquitin-ligase enzyme. The process of ubiquitin activation uses ATP as a substrate to the peptide bond formation between ubiquitin and E1. Then, the activated ubiquitin is transferred to an E2, which together with an E3 transfers ubiquitin to the substrate protein to be degraded by the proteasome (Callis, 2014). The E3 ubiquitin-ligase is believed to be the main responsible for substrate specific recognition and, to date, there are several E3 ligases already described. One such protein is the EC_5S (ElonginBC-Cullin5-SOCS) (Rodrigues *et al.*, 2009), which is a multi-subunit complex containing a scaffold protein (Cullin 5) attached to a RING finger protein (Rbx1)(Cullin 5-Rbx module), an adaptor heterodimer (Elongin BC), and a substrate recognition protein (suppressor of cytokine signaling [SOCS] box protein) (Cerqueira *et al.*, 2016). SOCS proteins share a 40-amino-acid sequence that is known as the SOCS-box motif, which is responsible for the interaction with Elongin BC and Cullin 5 modules establishing the bridge between the substrate of ubiquitination and the E2 ubiquitin-conjugating enzyme (Yoshimura, Naka and Kubo, 2007). The Elongin BC complex is a positive regulator of RNA polymerase II and has a transcriptionally active subunit A, and two regulatory subunits B and C. This complex has an important role in transcriptional regulation and acts as an adaptor connecting Cullin 5 and SOCS-box proteins (Okumura *et al.*, 2012) (Fig.3). Moreover, an Elongin BC complex containing a member of the Cullin RING ligase (CRL) superfamily plays a crucial role in some cellular processes such as tumorigenesis, signal transduction, cell mobility and differentiation (Okumura *et al.*, 2012).

Curiously, the LANA protein encoded by KSHV has a bipartite SOCS-box motif divided into a Cullin-box and a BC-box located within its C-terminal and N-terminal regions, respectively (Fig.2). This BC-box interacts with the host Elongin C creating a LANA-Elongin BC complex which is capable of assembling with a Cullin5/Rbx1 module and reconstitute a complex protein with E3

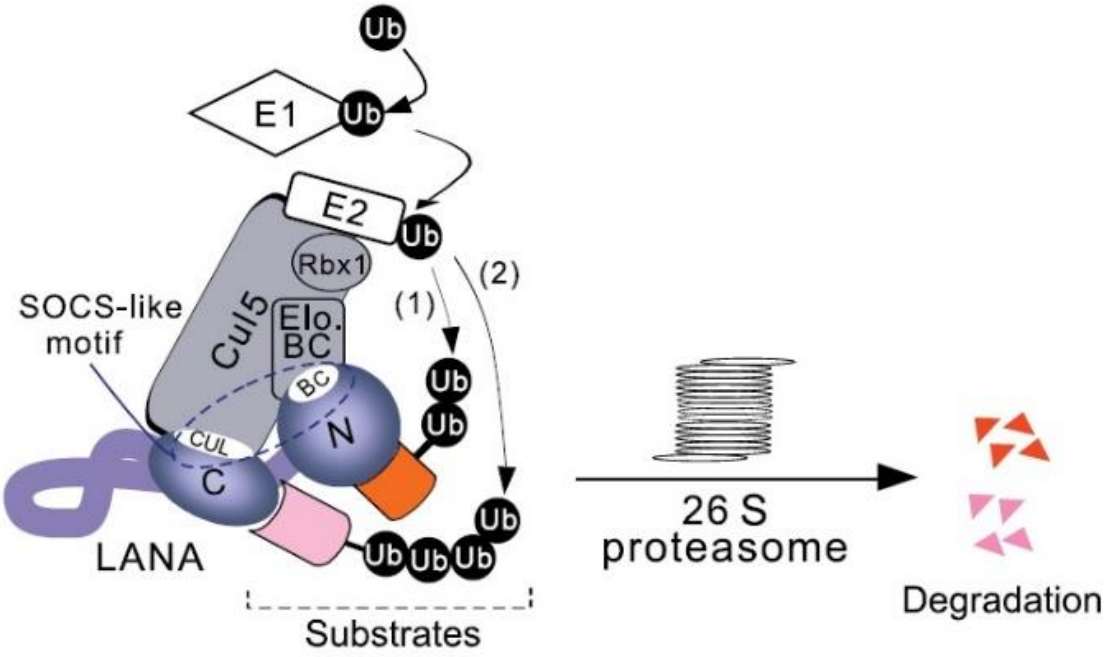

Figure 2 - A model for KSHV LANA assembles EC_5S ubiquitin complex to target downstream substrates for degradation. LANA is predicted to form a complex with Cul5/Rbx1 that interacts with Elongin BC. LANA acts as adapter to link substrates which bind at its amino (1) or carboxyl (2) -terminal domain (like VHL and p53) to EC_5S ubiquitin complex and induces the pathway of ubiquitin E1 activation, E2 conjugation, and substrate polyubiquitylation as well as 26S proteasome–mediated degradation (Cai *et al*., 2006).

ubiquitin-ligase activity (Cai *et al.*, 2006). This complex protein assembles an EC_5S ubiquitin ligase, which enables the virus to hijack the E3 ligase components of the cell, thus modulating the ubiquitination pathway of its host (Cerqueira *et al.*, 2016).

2.2 MHV68: a KSHV study model

The KSHV infection is naturally limited to humans, so it is of much importance to establish a small animal model of infection in order to study viral pathogenesis *in vivo* (Habison *et al.*, 2017). Dittmer *et al*., showed that KSHV infection into SCID mice implanted with human fetal thymus and liver grafts led to lytic and latent infection, mostly in B cells (Dittmer *et al.*, 1999). In 2006, Parsons and his team proved that injection into NOD/SCID mice resulted in latent and lytic infection in multiple cell types, including B cells and macrophages, for several months (Parsons *et al.*, 2006). Furthermore, oral, intraperitoneal or vaginal inoculation into a humanized NOD/SCID/IL2R gamma mouse implanted with human fetal liver and thymus also induced KSHV infection of both

B cells and macrophages (Wang *et al.*, 2014). However, despite the obvious advantage of allowing direct investigation of KSHV, these models are limited because they all require immune suppressed mice (Habison *et al.*, 2017). Thus, the deepest insights about KSHV biology mostly come from studying the murine gammaherpesvirus 68 (MHV68), a gamma-2 herpesvirus.

The MHV-68 is a naturally occurring virus that was first isolated from Slovakian bank voles (*Clethironomys glareolus*) and is endemic in European wood mice (Dong, Forrest and Liang, 2017). MHV68 genome consists of 118 kb, flanked by terminal repeat sequences of 1.2 kb and encodes approximately 80 genes (Pedro Simas and Efstathiou, 1998). This gammaherpesvirus is genetically related to KSHV and EBV and, a genomic organization showed that their genomes are collinear and contain large blocks of conserved genes (Pedro Simas and Efstathiou, 1998). Moreover, MHV68 is able to infect laboratory mice (*Mus musculus*) and establish a long persistent infection, contrarily to KSHV (Miranda *et al.*, 2018). Thus, MHV68 infection of mice provides a complementary, well-characterized model for KSHV investigation. It defines the distinction between establishment of latency and persistence of latency, which is the long-term survival of infected cells that are capable of reactivation upon the right stimuli (Dittmer *et al.*, 2016).

Following intranasal infection of mice, MHV68 undergoes acute productive (lytic) infection in the lungs and nasal epithelium (Dong, Forrest and Liang, 2017). During this phase, the virus replicates and disseminates progeny virions resolving by approximately 2 weeks post-infection (Purushothaman *et al.*, 2016; Dong, Forrest and Liang, 2017). After lytic infection in the lungs, MHV68 disseminates to lymphoid organs where it establishes latency and drives proliferation of the B cells germinal center in the spleen (Habison *et al.*, 2017). Latency is characterized by minimal viral gene expression and viral genome maintenance as an episome in the nucleus of the host cell (Purushothaman *et al.*, 2016).

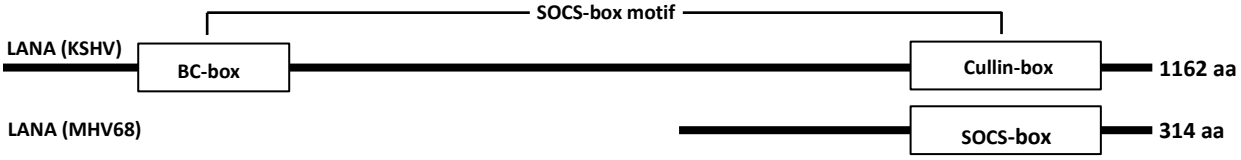

Figure 3- Schematic representation of LANA and ORF73. Proteins with the putative SOCS-box motifs indicated. The two proteins are aligned according to the shared primary sequence homology, corresponding to amino acids 95–274 and 963–1162 of ORF73 and LANA, respectively.

This viral infection model shares sequence homology and has a genome that is generally colinear with KSHV and, most importantly, it encodes a LANA homolog (mLANA). mLANA, despite being smaller than kLANA, has also a C-terminal DNA binding domain and is expressed in germinal center B cells (Virgin *et al.*, 1997; Habison *et al.*, 2017) (Fig.3). MHV68 LANA also mediates episome persistence by interacting with the TR sequences of the virus, which is

essential for efficient establishment of MHV68 latency *in vivo* (Correia *et al.*, 2013). Lastly, mLANA is also able to regulate transcription through E3-ligase activity by the assembly of an EC_5S complex which is mediated by a viral SOCS-box-like motif, homologous to the one present in the C-terminus kLANA (Correia *et al.*, 2013).

2.2.1 Chimeric virus – v-kLANA

In 2017, Aline C. Habison *et. al*, investigated the possibility of inter-species functionality between MHV68 and KSHV LANA for the investigation of KSHV persistent infection *in vivo*. They engineered a chimeric virus (v-kLANA) in which the mLANA was replaced with full-length kLANA ORF, including its 5´ untranslated region (UTR) (Fig.4). What they discovered was that kLANA was able to support episome persistence of plasmids containing TR elements from mLANA (mTR) and similarly, that mLANA can support episome persistence by acting with TR elements from kLANA (kTR) (Habison *et al.*, 2017). Moreover, they found that this chimeric virus, was capable of rescuing mLANA deficienct MHV68 and establish latent infection in mice. Finally, both wild type and chimeric MHV68 infected cells had similar viral genome copy numbers. These findings combined prove that mLANA and kLANA act reciprocally on TR DNA, and that kLANA functionally substitutes for mLANA, providing a novel infection model system for LANA investigation *in vivo* (Habison *et al.*, 2017).

2.2.2 Chimeric virus – v-KM

Both mLANA and kLANA have a C-terminal region that harbors a conserved DNA binding domain (DBD) that associates with TR DNA sequences and, along with other protein interactions, ensure the segregation and persistence of viral episomes during mitosis (Miranda *et al.*, 2018). However, the kLANA and mLANA DBDs differ in sequence and mode of oligomerization, which means that both proteins bind DNA in considerably different ways. mLANA oligomers bind DNA in a rigid and linear form, while kLANA oligomers are flexible and bent (Miranda *et al.*, 2018). Thus, Miranda *et. al*, generated a new chimeric MHV68 virus expressing kLANA with the C-terminal region of mLANA instead of that of kLANA. Indeed, this replacement resulted in a chimeric virus (v-KM) able to establish *in vivo* infection at higher levels compared with the previously described kLANA chimeric virus (v-kLANA) (Miranda *et al.*, 2018).

Significance

Despite more than 60 million years of evolutionary divergence between KSHV and MHV68, kLANA can functionally substitute for mLANA in MHV68 chimeric virus. kLANA is able to rescue mLANA deficient virus to enable a chimeric virus to establish latent infection in mice. This system allows *in vivo* investigation of kLANA in a well-established small animal model of infection.

In this project, both chimeric viruses (v-kLANA and v-KM) were used as a study model to assess KSHV infection *in vivo*. Viral mutations within the BC-box motif (T212A, L213A, N214A, P215A, I216A, C217A)) were engineered in order to achieve complete loss of E3-ubiquitin ligase without affecting episomal function, which lies in the C-terminus region of the protein.

Importantly, this work successfully tests the concept of functional substitution of a human pathogen gene into a model pathogen to allow *in vivo* investigation. Previously, such chimeric viruses were felt to be non-viable due to evolutionary divergence. These findings also have the potential to be applied to other human pathogens, which lack small animal models.

Chapter 2: Materials and Methods

1. Generation of MHV-68 recombinant viruses

1.1 Plasmids

pSP72_PCR1_3 (ampicillin resistance – ampR) contains DNA that encodes N-terminal kLANA (residues 123808-126473) and it's 5´UTR. This plasmid was constructed by Dr. Marta Miranda (Habison *et al.*, 2017).

pSP72_PCR1_3 Elo-BC (ampR) was generated in this project. It contains DNA encoding the same kLANA region as pSP72_PCR1_3, except for amino acid residues 212 to 217. Each of these residues was substituted for an alanine (g.212T>A, g.213L>A, g.214N>A, g.215P>A, g.216I>A and g.217C>A).

pSP72_PCR1_5 (ampR) contains DNA encoding the full length kLANA as well as its 5´UTR, flanked by MHV-68 sequences. This plasmid was constructed by Dr. Marta Miranda (Habison *et al.*, 2017).

pSP72_PCR1_5 EloBC (ampR) was generated in this project by subcloning a DNA fragment encompassing the mutations made in the pSP72_PCR1_3 Elo-BC (g.212T>A, g.213L>A, g.214N>A, g.215P>A, g.216I>A and g.217C>A) into the pSP72_PCR1_5 plasmid using BamHI/SacI restriction sites.

pSP72_994swap (ampR) contains DNA encoding the kLANA protein with the C-terminal region of mLANA in place of that same region of kLANA. This is a fusion protein in which the kLANA residues 1 to 994 were preserved and the C-terminal region (residues 995 to 1162) was replaced by the entire C-terminal mLANA (residues 118 to 314). This plasmid was also constructed by Dr. Marta Miranda (Miranda *et al.*, 2018).

pSP72_994swap EloBC (ampR) was generated in the course of this project by subcloning the DNA region encompassing the previous mutations made in the pSP72_PCR1_3 Elo-BC into the pSP72_994swap plasmid using BamHI/SacI restriction sites.

BamHI-G shuttle plasmid (kanamycin resistance – kanR) contains the MHV-68 genomic BamHI-G fragment (genomic coordinates 101653-106902) cloned into the pST76KSR plasmid, which is a shuttle vector. This plasmid was constructed by Dr. Sofia Marques. BamHI-G is the MHV-68 genome fragment that contains the mLANA coding sequence (genome coordinates 103925-104869).

BamHI-G shuttle_PCR1_5 Elo-BC (kanR) was generated during this project by subcloning the DNA region of pSP72_PCR1_5 EloBC between the two BglII sites. This subcloned plasmid

region contains DNA encoding the full length kLANA ORF (with the previously engineered mutations), its 5´UTR and an upper and lower flank of MHV68 sequences.

The BamHI-G Shuttle_994swap Elo-BC (kanR) was also generated during this project by subcloning the DNA region of pSP72_994swap EloBC between the two BglII sites. This subcloned plasmid region contains DNA encoding: the kLANA protein with the C-terminal region of mLANA in place of that same region of kLANA (with the previously engineered mutations); the 5´untranslated region as well as an upper and lower flanks of the MHV68 virus.

1.2 DNA: isolation and analysis

1.2.1 Plasmid DNA purification

All plasmid DNA was isolated from plasmid-containing *E.coli* strains (section1.3). Bacteria as grown in Luria-Bertani (LB) broth (NZYtech) containing the appropriate antibiotic and plasmid DNA was then isolated using an alkaline lysis method according to the scale of the preparation and known copy number of the plasmid.

Small scale plasmid preparations

For small scale plasmid preparations (minipreps), a single colony was inoculated in 10 mL of LB broth containing the appropriate antibiotic and incubated overnight with shaking (220 rpm) at 37°C. The next day cultures were centrifuged at 3059xg for 10min at room temperature (RT), and the pellet was processed using Promega's Wizard Plus SV minipreps DNA 13 Purification System, according to the manufacturer's instructions. Plasmid DNA was eluted in 70 μL of MiliQ nuclease free water and stored at -20°C.

Medium scale plasmid preparations

For medium scale plasmid preparations (midipreps), single colonies were inoculated in 50 mL of LB broth containing the appropriate antibiotic and incubated overnight with shaking (220 rpm) at 37°C or 30°C (for shuttle plasmid). The next day cultures were centrifuged at 6000 x g for 15 min at 4°C, and the pellet was processed using the QIAGEN Plasmid Purification kit, according to the manufacturer's instructions. Plasmid DNA was eluted in 100 μL of MiliQ nuclease free water and stored at -20°C.

Large scale plasmid preparations

For large scale plasmid preparations (maxipreps), single colonies were inoculated in 200 mL of LB broth containing the appropriate antibiotic and incubated overnight with shaking (220 rpm) at 37°C or 30°C (for shuttle plasmid). The next day cultures were centrifuged at 6000 x g for 10 min at 4°C, and the pellet was processed using the NZYTech NZYMaxiprep kit, using the manufacturer's instructions. Plasmid DNA was eluted in 150 μL of MiliQ nuclease free water and stored at -20°C.

1.2.2 Quantification and sequencing of DNA

DNA was quantified by ultraviolet spectrophotometry at 260 nm using a ND-2000 spectrophotometer (Thermo Scientific). When needed, in order to confirm if the desired DNA sequence was correct, DNA plasmid minipreps were sequenced at Eurofins using the Sanger method. The sequences were then analyzed with SnapGene 4.0.7 software.

Table 2 - Primers used for sequencing

OLIGONUCLEOTIDES	SEQUENCE (5´ – 3´)
F4 KLANA	CCGGGAATGCGCCTGAGGTCG
IMM TR8	ATCACCCCAGGATCCCTCAGAC
KLANA SEQ1	GTAAAGTAGGACTAGACAC

1.2.3 Restriction endonuclease reactions

Restriction endonuclease reactions were performed to obtain either inserts and/or linear vectors and for the screening of the correct clones after BAC mutagenesis. All reactions were performed using approximately 500-4000 ng of DNA and 1-20 U of restriction enzyme (New England Biolabs (NEB) or Roche) in a total volume of 30-50 µL and incubated for 1 hour (h) to overnight (O/N), at the temperature recommended by the manufacturer.

1.2.4 DNA ligation

For DNA ligations both vector and insert were digested, purified and ligated using T4 DNA ligase (NEB). Approximately 100 ng of vector DNA was ligated with 3-fold molar excess of insert vector in a 20 µL reaction containing 2 µL 10× T4 DNA ligase buffer, 1 U T4 DNA ligase and sterile MiliQ water. The reactions were incubated O/N at 16ºC and, in the next day, heat inactivated at 65°C for 10 minutes.

1.2.5 Analysis and isolation of DNA by gel electrophoresis

DNA fragments were separated by size on 0.8%-1.2% agarose (NZYTech) gels, in 1 × Tris Acetate-EDTA (TAE) buffer (40 mM Tris-acetate, 1 mM EDTA, pH 8.0) and DNA was stained with red safe (iNtRON Biotechnology) or gel red (Biotium). Loading buffer (10 mM EDTA, 5% glycerol, 0.025% bromophenol blue, 0.025% xylene cyanol) was mixed with the samples before loading them into the gel (1/10 of the final reaction volume). Electrophoresis was performed during 1 h to O/N, at 50 V to 100 V (Bio-Rad Laboratories power supplies), depending on the size of the DNA bands and on the assay. DNA fragments were visualized by UV transillumination, and images acquired using the ChemiDoc XRS$^+$ system. DNA fragments were further analyzed by comparison with the molecular weight ladder (1 kb Plus DNA Ladder, Invitrogen). In case of DNA band excision from gel, the DNA was purified using QIAquick gel extraction kit (QIAGEN), following the manufacturer's instructions. A small amount of purified DNA was analyzed on agarose gel to check DNA purification.

1.3 Bacterial strains

E. coli XL 10-Gold Ultracompetent Cells (Agilent Technologies) were used to transform the ligation reactions to obtain pSP72_PCR1_3 Elo-BC, pSP72_PCR1_5 EloBC and pSP72_994swap EloBC.

Competent *E. coli* DH5α prepared in the laboratory were used to transform ligation reaction to obtain the last two plasmids: BamHI-G shuttle_PCR1_5 Elo-BC and BamHI-G Shuttle_994swap Elo-BC, and to transform other plasmids, when needed.

E. coli DH10B, harboring the MHV68 cloned in a bacterial artificial chromosome (BAC), were provided by Dr. Heiko Adler and Dr. Ulrich Koszinowski (Adler *et al.*, 2000) and were used to generate the non-yfp recombinant viruses of this project.

E. coli DH10B yfp MHV68 BAC was kindly provided by Dr. Samuel Speck and were used to generate the yfp recombinant viruses. Collins *et. al*, cloned an expression cassette that expresses a fusion protein consisting of histone H2B and EYFP and cloned it into the region between ORFs 27 and 29b (Collins and Speck, 2012). This allows tracking of the MHV-68 infection of germinal center B cells *in vivo*.

1.3.1 Super Competent *E.coli* cells preparation

The desired *E. coli* strain was grown in LB broth medium with the required antibiotic selective pressure (ampicillin) at 18 °C, with shaking at 150-200 rpm until a final OD_{550nm} of 0.4-0.5 (24-36 hours). The next day cells were incubated on ice for 15 minutes and harvested by

centrifugation at 2000 xg for 15 minutes at 2 °C. The pellet was processed using the NZYTech NZYCompetent Cells preparation Buffer, under the manufacturer's instructions. Cells were aliquoted and stored at -80 °C.

1.3.2 Transformation of competent cells

E. coli XL 10-Gold Ultracompetent Cells were transformed according to the Agilent Technologies QuikChange Multi Site-Directed Mutagenesis Kit. Cells were gently thawed on ice and 45μL of the ultracompetent cells were distributed into a prechilled 15 mL falcon. 2 μL of β-Mercaptoethanol (provided with the kit), were added to each falcon tube and cells were incubated on ice for 10 minutes, swirling gently every 2 minutes. 1.5 μL of each mutagenesis reaction were added, and cells were incubated on ice for 30 min. The tubes were heat-pulsed in a 42 °C water bath for 30 seconds and then chilled on ice for 2 minutes. 500 μL of preheated Super Optimal Broth (SOC) (NZYTech) were added and cells were incubated for 1 hour with shaking at 220 rpm. Cells were spread on LB agar plates containing the appropriate antibiotic (100 μg/mL ampicillin, 30 μg/mL kan and/or 17 μg/mL cam) for the plasmid vector and incubated overnight at 37 °C.

E. coli DH10B and *E. coli* DH5α were transformed using the heat shock method. Cells were gently thawed on ice and approximately 10 ng of DNA were added per 100μL of cells. After incubation on ice for 30 minutes, cells were heat-shocked in a water bath for 45 seconds at 42 °C. 500 μL of SOC were added and cells were incubated for 1h at 37 °C or 30 °C (Shuttle plasmid) with shaking at 220 rpm. Cells were spread on LB agar plates containing the appropriate antibiotic (100 μg/mL ampicillin, 30 μg/mL kan and/or 17 μg/mL cam) for the plasmid vector and incubated overnight at 37 °C or 30 °C.

1.4 Cloning procedures to engineer v-kLANA Elo-BC and v-swap Elo-BC viruses

1.4.1 Mutagenesis: Polymerase Chain Reaction (PCR) to introduce mutations into pSP72_PCR1_PCR3

To introduce mutations into pSP72_PCR1_3 that change 6 amino acid residues in kLANA, a mismatch of 16 base pairs was required. Thus, to increase mutagenesis success, the mutagenesis strategy consisted in dividing it in two steps: first, nucleotides encoding the first 3 amino acids (mutagenesis 1) of the Elo-BC box kLANA (g.212T>A, g.213L>A, g.214N>A) were mutated to alanine and second, using this mutated plasmid, the remaining nucleotides (g.215P>A, g.216I>A and g.217C>A) (mutagenesis 2) were also mutated to alanine. The designed mutagenesis was performed using Agilent's QuikChange Multi Site-Directed Mutagenesis Kit.

Mutagenesis 1

PCR reaction, using the pSP72_PCR1_3 as template and iMM_APS1 as primer (Table 3), was performed. The iMM_APS1 primer is a mutagenic primer, designed specifically for this procedure (using the web-based QuikChange Primer Design Program), since it contains the desired mutations and the right sequence to anneal with the DNA present in the plasmid. The PCR reaction mix contained 10x QuikChange Multi reaction buffer, 200 µM of each deoxynucleotide (dNTP), 50 ng of each primer, 50 ng of DNA, 1 U of QuikChange Multi enzyme blend and MiliQ sterile water up to 25 µL. DNA was amplified on a thermocycler (Biorad) under the following condition parameters: an initial denaturation step at 95 °C for 1 minute followed by 30 cycles of amplification comprising 3 phases (denaturation at 95 °C for 1 minute, annealing at 55 °C for 1 minute and extension at 65 °C for 2 minutes/kb of plasmid length. 1 µL of methylation sensitive DpnI restriction enzyme (10 U/ µL), provided with the kit, was added to the amplification product and incubated at 37 °C for 1 hour to digest the parental (non-mutated methylated DNA) double stranded DNA (ds-DNA). Finally, the mutated single stranded DNA (ss-DNA) was transformed into *E. coli* XL 10-Gold Ultracompetent Cells, as described in section 1.3.2. The mutated plasmid was isolated from single colonies by small scale plasmid preparations (section 1.2.1) and the region encompassing the mutation was sequenced (section 1.2.2). Clone containing the mutations and no alterations elsewhere were selected for the second mutagenesis step – **clone 16** (which corresponds to pSP72_PCR1_3 plasmid encoding kLANA with g.212T>A, g.213L>A, g.214N>A).

Mutagenesis 2

Clone 16 was selected to proceed for the second and last part of the mutagenesis strategy. Therefore, it was subjected to a PCR reaction using iMM_APS2 primer (Table 3), also designed specifically for this procedure (using the web-based QuikChange Primer Design Program), since it contains the las 3 desired mutations and the right sequence to anneal with the DNA present in the plasmid. The PCR reaction mix was already described above, as well as the cycling parameters. The mutated single stranded DNA (ss-DNA) was transformed into *E. coli* XL 10-Gold Ultracompetent Cells, as described in section 1.3.2. The mutated plasmid was isolated from single colonies by small scale plasmid preparations (section 1.2.1) and the region encompassing the mutation was sequenced (section 1.2.2). The results were properly analyzed, and the right clones were selected in order to proceed with the cloning procedures – **clone 26** (which corresponds to pSP72_PCR1_3_Elo-BC, described in section 1.1).

Table 3 - Primers used in the mutagenesis strategy. Nucleotide mismatches are in red

OLIGONUCLEOTIDES	SEQUENCE (5´ – 3´)
iMM_APS1 (kLANA T212A, L213A, N214A)	GCGACTGACATATTGGGGCTGCTGCAGAGGGACCTTGGGGGGACGATAG
iMM_APS2 (kLANA P215A, I216A, C217A)	GAGACTGGGGGCGACTGAGCTGCTGCGGCTGCTGCAGAGGGACC

1.4.2 Subcloning the pSP72_PCR1_3 Elo-BC into pSP72_PCR1_5 and pSP72_994swap

pSP72_PCR1_3 Elo-BC (insert), pSP72_PCR1_5 (vector) and pSP72_994swap (vector) were digested with both BamHI (Roche) and SacI (Roche) restriction enzymes (section 1.2.3), and analyzed by gel electrophoresis to assess if the vectors and insert had the expected size. The desired fragments were cut from the gel and purified from gel with an appropriate kit (section 1.2.5). Insert and vectors were ligated (section 1.2.4) and the resulting reaction was transformed into competent DH5α cells (section 1.3.2). Each plasmid DNA was isolated from individual colonies by DNA miniprep and screened using the appropriate endonucleases. The resulting plasmids were: pSP72_PCR1_5 Elo-BC and pSP72_994swap Elo-BC (supplementary data, fig 1, A and B, respectively).

1.4.3 Subcloning pSP72_swap Elo-BC and pSP72_PCR1_5 Elo-BC into BamHI-shuttle vector

pSP72_PCR1_5 Elo-BC (insert), pSP72_994swap Elo-BC (insert) and BamHI-shuttle (vector) were digested with *Bgl*II (Roche) restriction endonuclease (section1.2.3). The DNA fragments were analyzed by gel electrophoresis and the corresponded bands were cut from the gel and finally purified, as mentioned. Ligation between inserts and vector was performed (section 1.2.4) and again the resulting reaction was transformed into competent DH5α cells (section 1.3.2). Each plasmid DNA was isolated from individual colonies by DNA miniprep and screened using the appropriate endonucleases. The resulting plasmids were: BamHI-G shuttle_PCR1_5 Elo-BC and BamHI-G Shuttle_994swap Elo-BC (supplementary data, fig.2, A and B respectively).

1.5 BAC mutagenesis

The MHV-68 recombinant viruses were generated by a Two-Step-Replacement strategy (Connor, Peifer and Bender, 1989) (supplementary data, fig.3).

BamHI-G shuttle_PCR1_5 Elo-BC and BamHI-G Shuttle_994swap Elo-BC were transformed into competent *E. coli* DH10B (section 1.2), from each background (yfp and non-yfp),

using the heat shock method (section 1.3.2). Bacteria were spread in LB plates containing both the selection marker of shuttle plasmid (kanamycin) and BAC (chloramphenicol). Plates were incubated 1-2 days at 30 °C. In this step a recombination event between homologous MHV-68 sequences in the BamHI-G recombinant shuttles and MHV-68 BAC takes place. This event is mediated by the RecA protein, which is encoded by the shuttle plasmid and enables the integration of the DNA contained in BamHI-G shuttle_PCR1_5 Elo-BC and BamHI-G Shuttle_994swap Elo-BC into the BAC genome, forming co-integrates. To select these co-integrates, 10 single bacteria colonies (from each background) were spread in LB plates containing kanamycin and chloramphenicol, concomitantly, and incubated overnight at 43 °C. In this step co-integrates are selected as the origin of replication for the shuttle plasmid is temperature sensitive. At 30 °C it can replicate, however at 42 °C the plasmid cannot replicate and its diluted out during growth. To ensure the selection of co-integrates this step was repeated. Next, the largest colonies were picked and plated on LB agar plates containing only chloramphenicol and incubated 1-2 days at 30 °C. In this step, co-integrates can resolve themselves by spontaneous homologous recombination to their initial condition or to the expected BAC mutant state. To isolate the resolved BAC mutants, 10 individual colonies (from each background, yfp or non-yfp) were streaked into LB agar plates, containing chloramphenicol plus 5% of sucrose (Sigma), which is a counter selection against the SacB gene, encoded by the BamHI-G shuttle plasmid. Plates were incubated 1-2 days at 30 °C. After, 5 clones from each plate (10 plates for each background, PCR Elo-BC yfp, PCR Elo-BC non-yfp, swap Elo-BC yfp and swap Elo-BC non-yfp) were picked and streaked in parallel: first in plates containing kanamycin and then on chloramphenicol plates, and incubated overnight at 37 °C. Being sucrose-resistant and kanamycin sensitive are two independent indicators that co-integrates are likely resolved. To identify the MHV68 BAC recombinants containing the kLANA mutants, two different colony PCR were performed: one for the mutants containing the full length kLANA mutants, using the primers LANA F1019 and LANA R1150 (upper and lower primers, respectively) that hybridize with the region encoding the C-terminal kLANA. Another colony PCR was used to detect the DNA encoding the N-terminal kLANA/C-terminal mLANA, using mLANAF_HindIII (upper) and kLANAF NruI (lower) primers that hybridize with the region encoding the N-terminal kLANA (Table 4). The PCR positive clones were grown in LB medium with 17 µg/mL of chloramphenicol and BAC plasmids were isolated by BAC minipreps (section 1.5.1) and further characterized by restriction profile analysis using EcoRI (NEBs), BamHI (Roche) and HindIII (Roche). Clones with the expected restriction profile were grown and BAC maxipreps were prepared (section 1.5.1).

Table 4 - Primers used in the colony PCR

OLIGONUCLEOTIDES	SEQUENCE (5´– 3´)
LANA F1019	GTCCCTTACAGACAGATAGATGATTG
LANA R1150	AAAAAGCTTTTATTCCCCTGGCTGGGTTAATG
mLANAF_HindIII	AAAAAGCTTGTGTACTTGTGGATGGCTG
kLANAF_NruI	CGAATACCGCTATGTACTCAGAACATC

1.5.1 BAC DNA preps

After the colony PCR analysis, the colonies that were positive were inoculated in 10 mL of LB broth with 17 µg/mL of chloramphenicol and grown O/N at 37 °C and 220 rpm. The next day, cells were centrifuged at 4000 rpm for 10 minutes, at 4 °C. BAC DNA was extracted by according to the alkaline lysis method followed by phenol/chloroform extraction. After discarding the supernatant, pellet was resuspended in 200 µL of buffer S1 (NucleoBond BAC 100 kit, Macherey-Nagel™) and 200 µL of buffer S2 (NucleoBond BAC 100 kit, Macherey-Nagel™) was added to lyse cells. The cell suspension was carefully mixed by inversion and incubated for 5 minutes, at room temperature (RT). 200 µL of pre-chilled buffer S3 (NucleoBond BAC 100 kit, Macherey-Nagel™) was added to neutralize the suspension, followed by a gentle mix by inversion and incubated for 15 minutes on ice. The suspension was then centrifuged for 15 minutes at 13000 rpm, at 4 °C, in order to separate the cell debris from the BAC DNA. The resulting supernatant was collected and transferred to a new tube where an equal volume of phenol:chloroform:isoamyl alcohol (25:24:1, Applichem A0944, 0250) was added, followed by a mixing step by inversion and incubation for 5 minutes at RT. Next, the mixture was centrifuged at 13000 rpm, at 4 °C and the aqueous phase was transferred to a new tube. 0.7 volumes of isopropanol (Sigma) were added and the mixture was mixed by inversion and incubated for 5 minutes at RT. To pellet the BAC DNA, tubes were centrifuged for 20 minutes at 4 °C, at 13000 rpm. After discarding the supernatant, the BAC DNA pellet was washed with 200 µL of 70% ethanol and centrifuged for 10 minutes, at 4 °C. Finally, after discarding the supernatant the pellet was air dried and resuspended in 60 µL of nuclease-free water and stored at 4 °C.

To successfully transfect cells, large amounts of pure BAC DNA are necessary. Thus, BAC DNA maxipreps were prepared from 300 mL of bacterial culture, grown O/N at 37 °C and shaking of 220 rpm. BAC DNA was purified and extracted using the NucleoBond BAC 100 kit (Machery-Nagel™), following the manufacturer's instructions.

To avoid damages to the BAC DNA, due to its large size, cut tips were used during the described protocols.

1.6 Cell lines

Mouse embryonic fibroblasts (NIH-3T3) expressing the CRE recombinase were used to remove the bacterial artificial chromosome (BAC) cassette (Stevenson *et al.*, 2002). They were cultured in Dulbecco's Modified Eagle Medium (DMEM) (Gibco® by life technologies) supplemented with 10% fetal bovine serum (FBS) (Gibco® by life technologies), 100 U/mL penicillin-streptomycin (Gibco® by life technologies) and 2mM L-glutamine (Gibco® by life technologies).

Baby hamster kidney fibroblast (BHK-21) (clone C3) cells were used to grow and titrate viral stocks, for plaque assays and *ex vivo* reactivation. They were maintained in Glasgow Minimum Essential Medium (GMEM) (Gibco® by life technologies) supplemented as described above, plus 10% tryptose phosphatase broth (TPB) (Sigma).

Both cell cultures were maintained in a humidified tissue culture incubator at 37 °C with 5% CO_2.

1.7 Viruses

In this study two non-yfp control viruses were required, and 8 MHV68 recombinant viruses were constructed (Table 5). However, only the non-yfp viruses were used to inoculate mice, as described below.

Control viruses

v-kLANA is a chimeric kLANA MHV-68 virus, in which mLANA was replaced by the full length kLANA, and it's 5'UTR. It was constructed by Dr. Marta Miranda (Habison *et al.*, 2017) and was used as a control virus for the v-kLANA Elo-BC viruses.

v-KM is a chimeric virus containing a fusion protein between kLANA and mLANA. This virus contains the full length kLANA but with the C-terminal region of mLANA. Thus, the DNA binding domain (DBD) of this virus belongs to mLANA, resulting in a more efficient infection in mice, as published in (Miranda *et al.*, 2018). v-KM was constructed by Dr. Marta Miranda and was used as a control virus for the v-KM Elo-BC viruses.

MHV-68 recombinant viruses

v-kLANA Elo-BC clone 32 and v-kLANA Elo-BC clone 46 are chimeric kLANA MHV68 viruses, in which mLANA was replaced by the full length kLANA Elo-BC and it's 5'UTR. Engineered Elo-BC mutations alter residues T212A to C217A, as described in section 1.4.

v-KM Elo-BC clone 32 and v-KM Elo-BC clone 34 are chimeric virus that contain a fusion protein between kLANA and mLANA. They also contain the previously engineered mutations in the amino acid residues T212A to C217A, already described in section 1.4.

Table 5 - List of MHV68 recombinant virus constructed during this project

MHV68 recombinant virus name	Virus features
v-kLANA Elo-BC 32	Chimeric kLANA MHV-68 viruses, in which mLANA was replaced by the full length kLANA and it's 5'UTR. These viruses contain the engineered mutations in the amino acid residues 212 to 217 and are genetic clones. Both viruses were generated through BAC mutagenesis through a transformation using *E. coli* DH10B.
v-kLANA Elo-BC 46	
v-kLANA Elo-BC 7.4-yfp	Chimeric kLANA MHV-68 viruses, in which mLANA was replaced by the full length kLANA and it's 5'UTR. These viruses contain the engineered mutations in the amino acid residues 212 to 217 and are genetic clones. Both viruses were generated through BAC mutagenesis through a transformation using *E. coli* DH10B carrying an yfp tag, allowing tracking of MHV68 infection of GC B cells *in vivo*.
v-kLANA Elo-BC 8.5-yfp	
v-KM Elo-BC 32	Chimeric viruses that contain a fusion protein between kLANA and mLANA. These viruses contain the full length kLANA but with the C-terminal region of mLANA. They contain the previously engineered mutations in the amino acid residues 212 to 217. Both viruses were generated through BAC mutagenesis through a transformation using *E. coli* DH10B.
v-KM Elo-BC 34	
v-KM Elo-BC 8.4-yfp	Chimeric viruses that contain a fusion protein between kLANA and mLANA. These viruses contain the full length kLANA but with the C-terminal region of mLANA. They contain the previously engineered mutations in the amino acid residues 212 to 217. Both viruses were generated through BAC mutagenesis through a transformation using *E. coli* DH10B carrying an yfp tag, allowing tracking of MHV68 infection of GC B cells *in vivo*.
v-KM Elo-BC 9.5-yfp	

1.8 Reconstitution of MHV-68 viruses

1.8.1 Virus reconstitution on BHK-21 cells

MHV-68 viral reconstitution from genomic DNA was performed on BHK-21 cells. On the day before the transfection, cells were seeded at $1x10^6$ cells/6 cm^2 dish. The next day, with DNA, unsupplemented GMEM and the X-tremeGENE HP DNA Transfection Reagent (Roche) at RT, 1 μg of BAC DNA maxiprep was diluted into 500 μL of unsupplemented GMEM (using a cut tip) in an eppendorf. Next, 2 μL X-tremeGENE HP DNA Transfection Reagent were added into the media and mixed gently, followed by an incubation of 20 minutes at RT. Each transfection complex was added to the cells and incubated at 37 °C until a cytopathic effect (CPE) was

observed (approximately 4 days). Finally, cells were scraped onto media, harvested and stored at -80 °C (BAC+ viral stocks).

1.8.2 Passage through NIH3T3-Cre cells to remove BAC sequences

The BAC cassette is flanked by *lox*P sites and, among others, contains a green fluorescence protein (GFP) gene (Adler *et al.*, 2000, 2001), making possible the screening of virus containing this gene through a GFP marker. Therefore, BAC+ viral stocks were passed through NHI3T3-Cre cells to remove the entire BAC sequence (between loxP sites). This protocol enables the viruses to gradually loose the GFP signal in each passage, meaning losing the BAC cassette (supplementary data, fig.4).

One day before infection, $1.75x10^5$ cells/well were seeded in 6-well plates and the BAC cassette was removed by cell passage coupled with limiting dilutions. When the GFP signal was no longer observed, using a fluorescence microscope, cells were scrapped, harvested and stored at -80 °C (BAC- viral stocks). These were the viral stocks used to produce the working stocks, as described below in section 1.8.

1.9 Production of viral stocks: working stock media (WSM) and cell working stock (CWS)

Viral working stocks were produced from BAC- viral stocks, by infecting $5x10^6$ BHK-21 cells in 175 cm^2 flasks, at a low multiplicity of infection (MOI): 0.002 plaque forming units (PFU)/cell. After infection, cells were incubated for 4 days at 37 °C. Following incubation, cells were scrapped into supplemented GMEM and centrifuged at 1500 rpm for 5 min, at 4 °C. The supernatant was transferred into 30 mL bottles and centrifuged at 15000 xg, for 2h at 4 °C and the cell pellet was resuspended in 2 mL of complete GMEM, aliquoted and stored at -80 °C (Cell Working Stock – CWS). Next, the supernatant was discarded, the pellet was resuspended in 2 mL GMEM, aliquoted and stored at -80 °C (Working Stock Media – WSM).

1.10 Virus titration using the suspension method: plaque assay

Titration of viruses was performed using the suspension method in BHK-21 cells. 10 μL of virus was added to a 15 mL falcon tube, already containing 990 μL of supplemented GMEM, diluting the virus 100 times (10^{-2}) and then 10-fold serial dilutions were made (10^{-3} to 10^{-8}). Next 1 mL of $2.5x10^5$ BHK-21 cells were added to each falcon and incubated in a rotating table (30 rpm) for 1 h at RT. Following the incubation period, 2 mL of supplemented GMEM was added and, after mixing falcons by inversion, cells were added to 6-well plates and incubated for 4 days

at 37 °C. Four days later, media was removed, and cells were fixed with 4% formaldehyde in PBS, for 10 minutes and stained with 0.1% toluidine blue, for 5 minutes. Viral plaques were counted using a magnifying glass. Finally, all titers were calculated according to the following formula:

$$Virus\ titer = n^{o}\ of\ plaques \times \frac{1}{dilution} \times \frac{1}{inocolum}$$

2. Protein expression analysis

To detect expression of kLANA protein in the control viruses and in the recombinant MHV-68 viruses generated in this project, BHK-21 cells were infected with: v-kLANA Elo-BC 32, v-KM Elo-BC 34, v-kLANA and v-KM. On the day before the infection, BHK-21 cells were seeded in 12-well plates ($2x10^5$ cells/well), followed by infection with a MOI of 3 (3 PFU/cell) in a total volume of 500 μL, in the next day. As an uninfected control, well was incubated with 500 μL of supplemented GMEM. After de inoculation, cells were incubated for 2 hours, at 37 °C with gentle rocking every 30 min. Next, the inoculum was removed, and the cells were gently washed with 1 mL of pre-heated supplemented media and 1 mL of fresh supplemented media was added. Following the 4 hour incubation period, at 37 °C, cells were washed twice with ice cold PBS and 60 μL of lysis buffer (20 mM Tris-HCl pH 7.4, 150 mM NaCl, 1 mM Na3VO4, 1 mM NaF, 1% TritonTM X-100, protease inhibitors (Roche), miliQ H2O) was added to each well. Cells were harvested into an eppendorf, incubated on ice for 10 min and centrifuged at 13000 rpm (to remove cell debri) for 10 min at 4 °C. Finally, the supernatant was transferred into a new tube and 50 μL of 2xLaemmelli's buffer (100 mM Tris-HCl pH 6.8, 20% glycerol, 4% SDS, 10% β-mercaptoethanol) were added to the cell lysates and frozen at -20 °C until further use. Before loading the samples into a polyacrylamide gel, samples were heated at 95 °C for 3 min in a heat block.

2.1 Sodium dodecyl sulfate-polyacrylamide gel electrophoresis (SDS-PAGE)

The protein samples were separated by SDS-PAGE, in 1.5 mm mini-slab gels (BioRad). The stacking gel used had a percentage of 5% polyacrylamide, 1.0 M Tris-HCl (pH 6.8), 10% SDS, 10% ammonium persulfate and tetramethylethylenediamine (TEMED) (Sigma). The resolving gel had a percentage of 10 % polyacrylamide (Acrylamide:bis-acrylamide 37.5:1, BioRad), 1.5 mM Tris-HCl (pH 8.8), 10% SDS (BioRad), 10% ammonium persulfate and TEMED.

After the polymerization of gels, 50 μL of each protein sample and 5 μL of molecular weight marker (Dual color, BioRad) were loaded into the gel. The electrophoresis was performed at 180 V constant, in 1xTGS buffer (25 mM Tris, 192 mM glycine and 0.1% SDS), for 1 h.

2.2 Transference of proteins into nitrocellulose membranes

After protein separation, proteins were transferred from the gels to nitrocellulose membranes (GE Healthcare) by the wet-transfer method. The transference was performed at 100 mA, O/N, at 4 °C and was carried out in 1xTG buffer (25 mM Tris, 192 mM glycine, 20% methanol) (BioRad) and 0.1% SDS. To confirm the protein transfer nitrocellulose membranes were incubated with Ponceau S dye (Sigma) for 2 min. Before proceeding with the protocol, dye was removed from the membrane by incubation with wash buffer (PBS+0.05% Tween-20).

2.3 Western blot

The membrane was incubated with blocking solution (5% non-fat powder milk in wash buffer) on a rotating table for 30 min, 10 rpm at RT. Membranes were washed twice and incubated, in a rotating table (10 rpm), with the primary antibody (Table 6) diluted in blocking buffer, in sealed bags (1 h, RT). Next, membranes were washed 3 times and incubated with the blocking solution containing the secondary antibodies (Table 6) for 30 min on a rotating platform (10 rpm, RT). Finally, membranes were washed 3 times and detection of protein-antibody complexes were performed by chemiluminescence using SuperSignal® West Pico Chemiluminescent Substrate (Thermo Scientific), according to the manufacturer's instructions. The capture and analysis of the protein-antibody complexes was performed using Amersham™ Imager 680.

Table 6 - Antibodies used in the western blot assay

Antibodies	Name (antigen)	Species	Dilution	Company
Primary	LN53 (kLANA)	Rat	1:1000	Advanced Biotechnologies
	Actin (actin)	Rabbit	1:1000	Sigma
Secondary	Anti-rat	Goat	1:5000	Jackson Immune research
	Anti-rabbit	Donkey	1:5000	Jackson Immune research

3. Ethics statement

This study was performed in strict accordance with the recommendations of the Portuguese National Authority for Animal Health (Portaria 1005/92). The Portuguese Experiments on Animal Act complies with the European Directive 2010/63/EU and follows the Federation of European Laboratory Animal Science Associations (FELASA) guidelines on laboratory animal welfare.

4. Mice

Female BALB/cByJ mice (6-8 weeks old) were purchased from Charles Rivers Laboratories. Animals were housed and subjected to experimental procedures in specific pathogen-free conditions, at Instituto de Medicina Molecular João Lobo Antunes animal facility, Lisbon, Portugal.

5. In vivo assays

5.1 Infection of mice

Mice were divided into 4 groups of infection, with 16 mice each, according to the virus that was inoculated (v-kLANA, v-KM, v-kLANA Elo-BC 46 or v-KM Elo-BC 34) and were sacrificed at five different time points post-infection (Table 7). Animals were briefly anaesthetized with isoflurane and were intranasally inoculated with 10^4 PFU in 20 μL of PBS. At each time point, mice were sacrificed by isoflurane overdose and lungs and/or spleens were collected. Five days post infection (dpi) 4 mice of each group were sacrificed, and lungs were collected to a falcon containing 5 mL of supplemented GMEM. Seven dpi, 4 mice of each group were sacrificed, and lungs were collected to a falcon containing 5 mL of supplemented GMEM. Ten days post-infection, 4 mice of each group were sacrificed and both lungs and spleen were collected to a falcon containing 5 mL of supplemented GMEM. At day 14 and 21 post infection, another 4 mice of each group were sacrificed, and only spleens were collected to falcons containing 5 mL of supplemented GMEM.

Table 7 - *in vivo* experiments

	0 dpi	5 dpi	7 dpi	10 dpi	14 dpi	21 dpi
Virus	Nº of mice	Number of collected organs (per infection group)				
		Lungs	Lungs	Lungs + spleens	Spleens	Spleens
v-kLANA	20	4	4	4 + 4	4	4
v-kLANA Elo-BC 46	20	4	4	4 + 4	4	4
v-KM	20	4	4	4 + 4	4	4
v-KM Elo-BC 34	20	4	4	4 + 4	4	4
Total	80	16	16	16 + 16	16	16

5.2 Lung viral titration

Lungs were homogenized in supplemented GMEM, using a glass homogenizer, and frozen at -80 °C in order to lyse cells. Next, viruses were diluted through serial 10-fold dilutions in 1 mL of supplemented GMEM. Hence, 10 μL of each virus was added to an eppendorf with 990 μL of supplemented GMEM (10^{-2} dilution). After vortexing the tube, 100 μL were added to the first 15 mL falcon, already containing 900 μL of supplemented GMEM (10^{-3} dilution) and, following vortex, one more serial dilution was made (10^{-4} dilution). Dilutions were always performed in duplicate. Lung viral titration of lungs from 10 dpi mice was performed using the neat (undiluted suspension), 10^{-1} and 10^{-2} dilutions. Once the dilutions were completed, 1 mL of BHK-21 cells ($5x10^5$ for 6 cm dishes or $2.5x10^5$ for 6-well plates) were added to each tube and incubated in a rotating table for 1 h, at RT, 30 rpm. Following the incubation period, 2 mL of supplemented media was added to each falcon, then mixed by inversion and plated into 6 cm cell culture dishes or 6-well plates. Viral plates or dishes were incubated for 4 days, at 37 °C. After the incubation period, cells were fixed with 4% formaldehyde in PBS, for 10 minutes and stained with 0.1% toluidine blue, for 5 min. Viral plaques were counted using a magnifying glass and the PFU/lung was calculated according to the formula described in section 1.10.

5.3 Single cell suspensions

In order to prepare single cell suspensions, spleens were homogenized with a syringe plunger and filtered through a 100 μm cell strainer to remove cell debris. Cells were centrifuged at 1200 rpm, for 5 min at 4 °C and the pellet was resuspended in 1 mL of Red Blood Lysis buffer (RBL) (154 mM ammonium chloride, 14 mM sodium hydrogenate carbonate, 1 mM EDTA pH 7.3). After incubating the pellet on ice for 5 min, 5 mL of complete GMEM were added and another

centrifugation was performed at 1200 rpm, for 5 min at 4 °C. The new pellet was resuspended in 1 mL of media and then 4 mL of complete GMEM were added, resulting in a single cell suspension of 5 mL. This suspension was used to determine the viral latency by infectious center assay (ICAS) and the frequency of viral DNA positive cells by limiting dilution assay.

5.4 Infectious Center Assay (ex vivo explant co-culture assay)

To assess viral latency, virus titers were determined by reactivation assay in BHK-21 cells. 1mL of the splenocyte suspension was added to 6 cm dish (neat or 10^{-1} dilution), in duplicate. Each plate already contained 1 mL of $4x10^5$ cells and media up to 5 mL, and were incubated for 5 days at 37 °C. In parallel, spleens were also screened for the presence of pre-formed infectious viruses. Undiluted splenocyte suspensions were freeze-thawed, plated, in duplicate, and incubated for 4 days, at 37 °C. After the incubation period of both assays, cells were fixed with 4% formaldehyde in PBS, for 10 minutes and stained with 0.1% toluidine blue, for 5 min. Viral plaques were analyzed and counted using a magnifying glass and infectious centers (PFU/spleen) were determined, according to the formula in section 1.10.

5.5 Limiting dilution assay and real-time PCR of viral DNA positive cells

To determine the frequency of viral DNA positive cells, a 1 mL splenocyte pool, for each infection group, was prepared from single cell suspensions from individual mice. Then the pool was centrifuged at 1300 rpm, for 5 removed with a tip and filtered through a 40 μm cell strainer. Cells were counted and diluted at $2x10^6$ cells in 100 μL of 2% FBS/PBS, and subsequent serial 2-fold dilutions were made in 2% FBS/PBS. 5 μL of each performed dilution were added to PCR tubes already containing 10 μL of lysis buffer (10 mM Tris-HCl, 3 mM, MgCl2, 50 mM KCl, 0.45% NP-40, 0.45% Tween-20, 0.5 mg/mL Proteinase K). All PCR tubes were incubated O/N at 37 °C and, in the following day, proteinase K was inactivated by heating cell lysates to 95 °C for 5 min, in a thermocycler. Tubes were stored at -20 °C until further use.

Cell lysates were analyzed by real time PCR on Rotor Gene 6000 (Corbett Life Science) using a fluorescent Taqman probe and specific primers for MHV-68 M9 gene: M9-F (upper primer): 5'-GCCACGGTGGCCCTCTA-3', M9-R (lower primer): 5'-CAGGCCTCCCTCCCTTTG-3' and M9-T probe: 5'- 6-FAM-CTTCTGTTGATCTTCC-MGB-3'. PCR reactions were prepared in a total volume of 25 μL, containing 200 nM of each primer, 1x mix (Invitrogen), 300 nM of probe, 5 mM of $MgCl_2$, nuclease-free water plus 2.5 μL of each cell suspension lysate. Water was used as a negative control and pGBT9-M9 plasmid, as a positive control. The cycling program

consisted of an initial melting step of 95 °C, for 10 min followed by 40 cycles of amplification: 95 °C for 15 seconds and then 60 °C for 1 min. The results were analyzed using the Rotor Gene 6000 software and each sample was scored either positive or negative by comparison to negative and positive controls. Frequency of viral DNA positive cells was calculated from a regression plot of input cell number against the fraction of negative sample described by Dr. Sofia Marques (Marques *et al.*, 2003).

6. Statistical analysis

Statistical analysis was performed with GraphPad Prism Software, by Mann-Whitney test. For limiting dilution analysis, 95% confidence intervals were determined as described (Marques *et al.*, 2003).

Chapter 4: Results and Discussion

1. Generation and characterization of MHV68 recombinant virus

The BC-box encoded by kLANA in its N-terminal region interacts with the host Elongin C creating a LANA-Elongin BC complex which is capable of assembling with a Cullin/Rbx1 module and reconstitute a complex protein with E3 ubiquitin-ligase activity. Indeed, this E3 ubiquitin-ligase activity is thought to be essential for latency maintenance (Rodrigues *et al.*, 2009). Thus, recombinant chimeric viruses with engineered mutations within the BC-box (T212A, L213A, N214A, P215A, I216A, C217A) of kLANA were generated using MHV68 chimeric model of infection to assess viral latency *in vivo* (Fig.4).

After a two-step strategy to successfully mutate the BC-box, another two steps of cloning were necessary in order to obtain the entire kLANA ORF, with the engineered mutations, cloned into a shuttle vector (supplementary data fig.2). The chimeric viruses (v-kLANA Elo-BC and v-KM Elo-BC) were generated in two MHV68 genomic backgrounds (yfp and non-yfp) through a mutagenesis procedure in *E.coli* DH10B harboring a BAC plasmid with the MHV68 genome cloned, according to a Two-Step-Replacement strategy (Connor, Peifer and Bender, 1989).

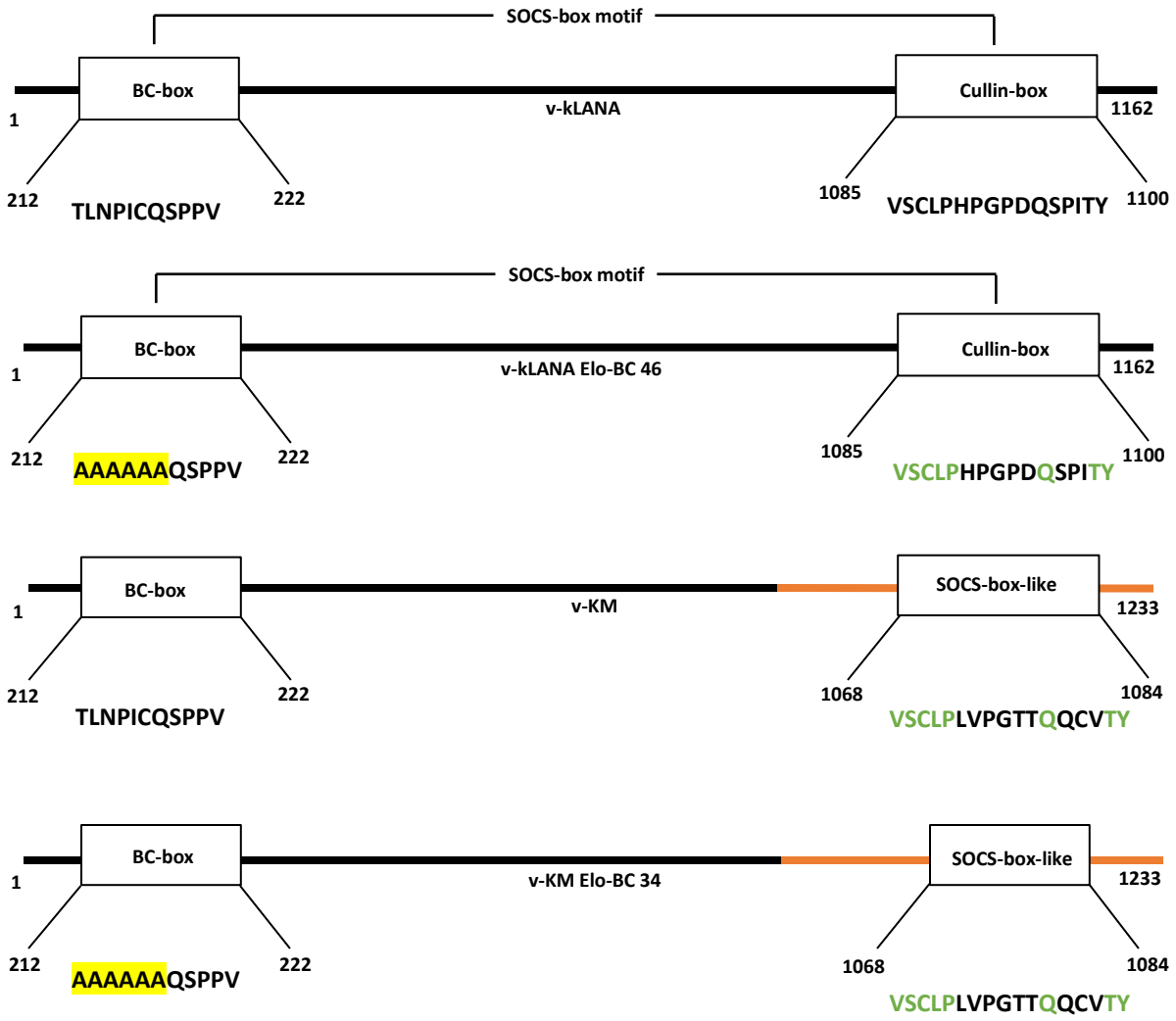

Figure 4 - Representation of kLANA proteins expressed by each virus, highlighting the kLANA SOCS-box motif. v-kLANA has the wild type kLANA ORF, with the N-terminal region and the C-terminal region with the BC-box and Cullin-box, respectively. v-kLANA Elo-BC 46 mutant is the same as v-kLANA but with the engineered mutations in the BC-box (in yellow). v-KM encodes the full length kLANA but with the C-terminal region of mLANA (in orange), including its SOCS-box-like motif. v-KM Elo-BC 34 is the same as v-KM but with the engineered mutations in the BC-box (in yellow). Identical amino acids are in green.

After mutagenesis procedures in DH10B *E.coli* (supplementary data fig. 3), colony PCR was performed to identify the MHV-68 BAC recombinants containing kLANA mutants replacing the MHV68 mLANA. Positive clones were grown. After BAC DNA extraction, clones were analyzed by restriction digestion with EcoRI (Fig.5). Clones containing the correct restriction profile were selected to prepare high quality maxiprep BAC DNA, and genome integrity was assessed once more by restriction digestion using two different endonucleases: EcoRI and BamHI (Fig.5), using v-kLANA, v-KM and v-WT BAC DNA as controls. Two independent clones from each virus depicting no gross genomic alterations (Fig. 5) were selected and transfected into BHK-21 cells for viral reconstitution. The BAC cassette, flanked by loxP sites, was excised

through the Cre-lox system by infection of NIH-3T3 cells expressing Cre recombinase (Fig.6). BAC$^-$ viral stocks were obtained for all non-yfp and yfp viruses, but only the non-yfp viruses were selected to move forward in the project.

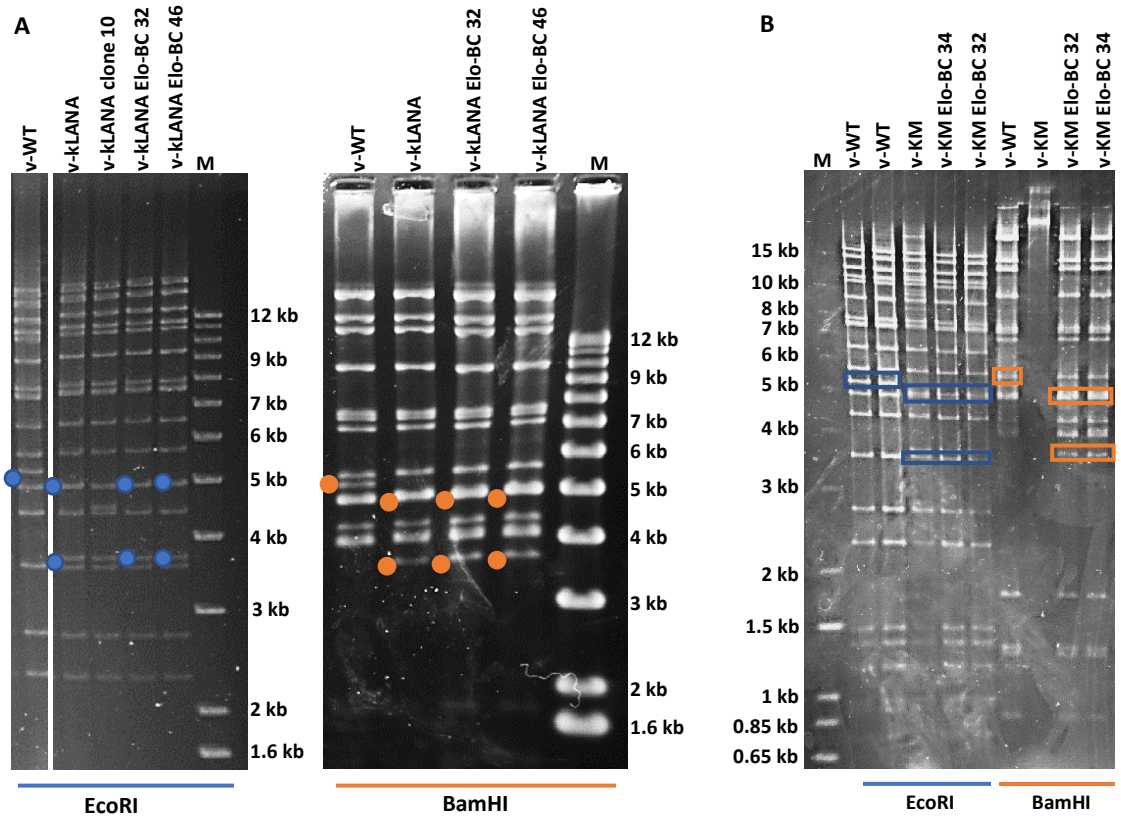

I

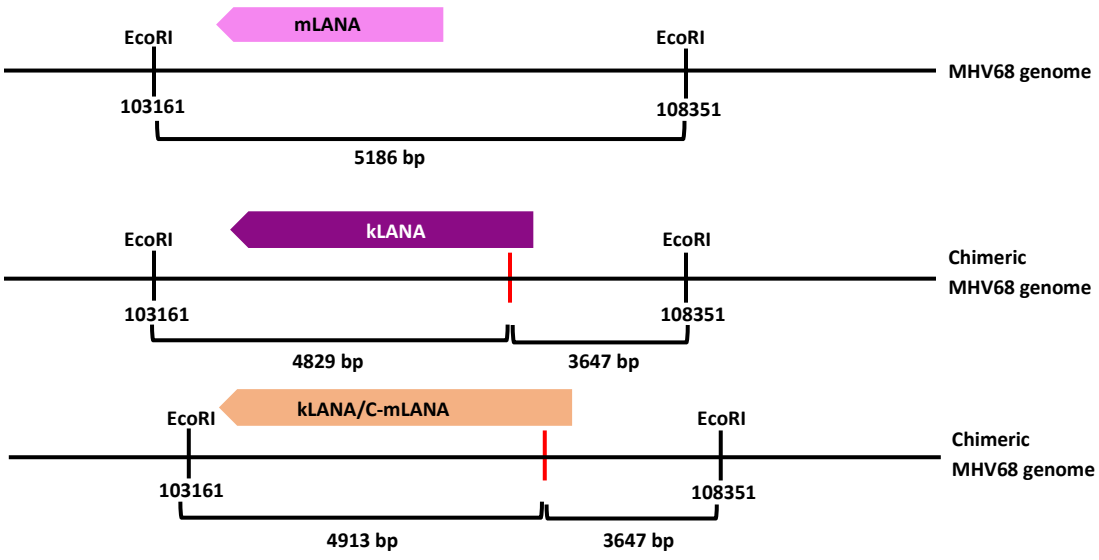

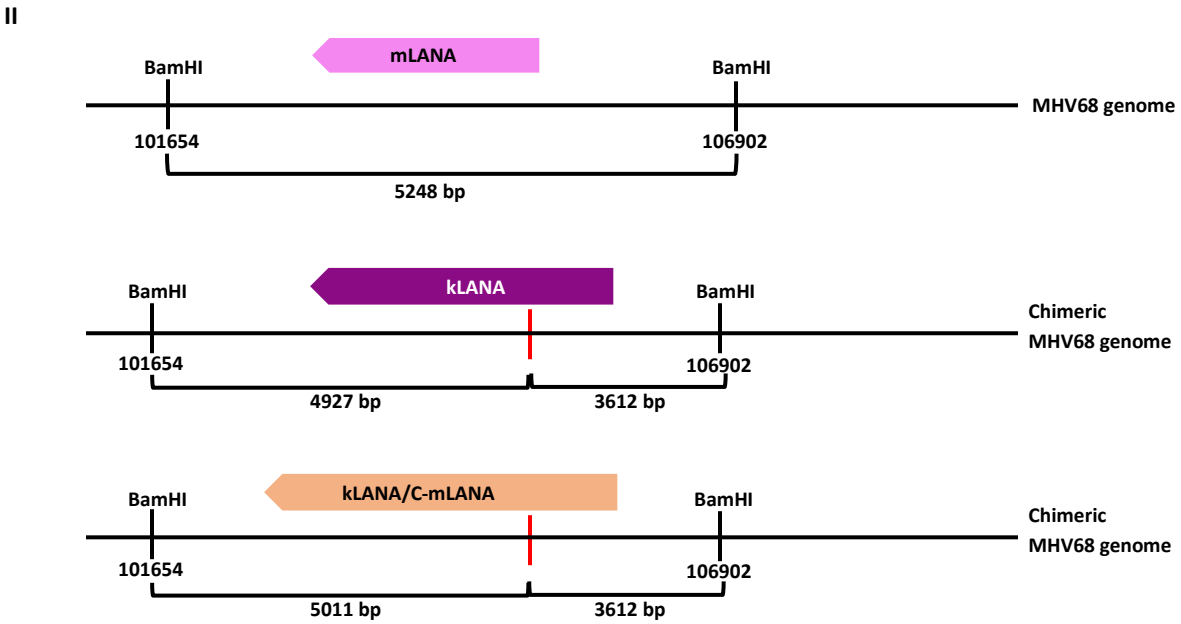

Figure 5 - Restriction profiles of non-yfp BAC plasmids and schematic representation of MHV68 genome with each restriction enzyme sites. A) Restriction profile analysis of v-WT, v-kLANA and v-kLANA mutants using EcoRI and BamHI (blue and orange respectively). Molecular weight is indicated on the right. B) Restriction profile analysis of v-WT, v-KM and v-KM mutants using EcoRI and BamHI (blue and orange respectively). Molecular weight is indicated on the left. (I) EcoRI restriction sites. (II) BamHI restriction sites. Introduced restriction sites are in red.

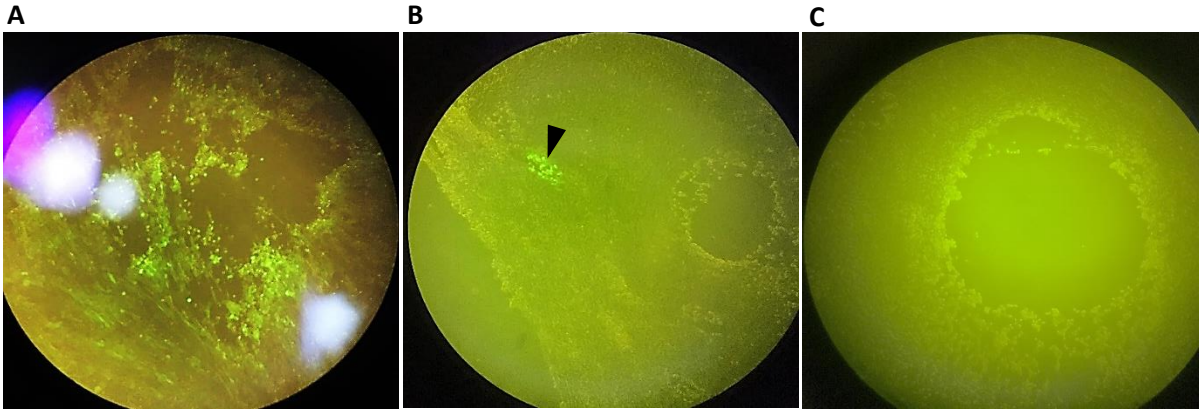

Figure 6 - BAC cassette removal through NHI-3T3 cells expressing Cre recombinase. A) passage 1, cells exhibit a strong GFP signal, B) passage 2, GFP signal is weaker (black arrow indicates the remaining cells with the BAC cassette expressing GFP) and C) passage 3, no GFP signal detected

2. In vitro assays

2.3 Viral titration

Calculating the exact viral concentration in viral stock is essential to perform both *in vitro* and *in vivo* experiments. Thus, each viral stock was titred and the concentrations are shown in

table 8. All viral stock concentrations were within the normal range value obtained in the laboratory (>10^6 PFU/mL).

Table 8 - Viral stock titers

Virus	Titer (PFU/mL)
v-kLANA	$2.22x10^7$
v-KM	$2.11x10^7$
v-kLANA Elo-BC 46	$2.22x10^7$
v-KM Elo-BC 34	$1.11x10^7$

2.4 Expression of kLANA mutant proteins

To investigate if all the recombinant viruses expressed kLANA proteins, an immunoblot was performed. BHK-21 cells were infected with each virus at a MOI of 3 PFU/cell during 6h and total cell lysates were prepared and analyzed using specific antibodies against kLANA and other cellular proteins. LN53 is a commercial antibody that recognizes the EQEQ glutamic motifs found in the glutamate and glutamine internal repeat region (EQE) of kLANA. All mutants and control viruses presented the full length kLANA with a molecular weight of approximately 250 kDa and lower molecular weight isoforms (Fig.7). Hence, the engineered mutations did not affect kLANA expression. Actin protein is commonly used as a loading control, since it is present in all eukaryotic cells. All infected cells and the mock uninfected cells presented identic levels of actin, detected at approximately 42 kDa, indicating equivalent loading of samples (Fig.7).

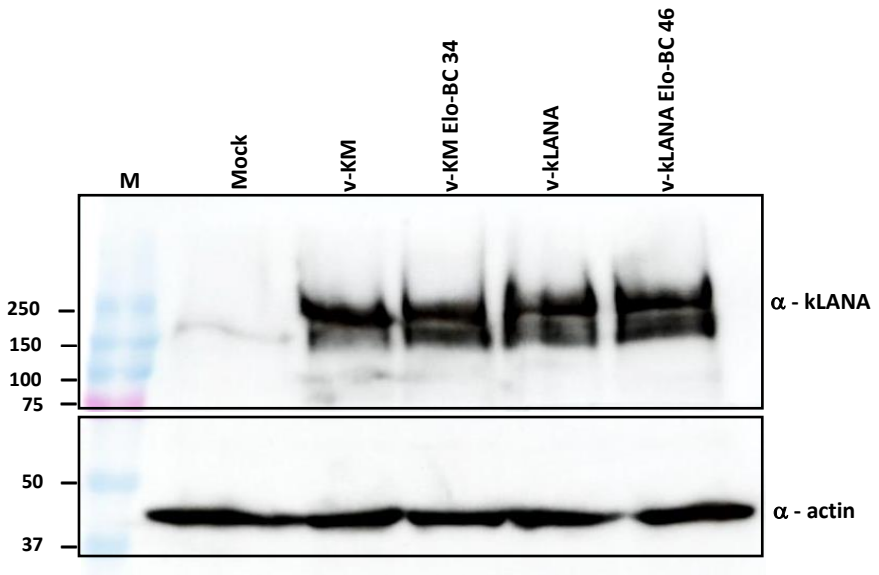

Figure 7 - **Expression detection of viral protein kLANA.** BHK-21 cells were infected with 3 PFU/cell during a period of 6h. The proteins were detected with the antibodies indicated on the right and the molecular weight protein markers are indicated on the left.

3. In vivo assays

The role of the introduced mutations in kLANA BC-box was then characterized in a natural context of infection of mice by analysis of the acute phase of infection in lungs and latency in spleens, comparing the values of infection with the control viruses (v-kLANA and v-KM).

3.1 Lung viral titers

During the first days after intranasal infection, MHV68 virus undergoes acute lytic infection in the lungs and, during this phase, the virus replicates and disseminates progeny virions. Lung lytic infection is resolved by approximately 10 days post-infection (Purushothaman *et al.*, 2016; Dong, Forrest and Liang, 2017). Thus, by lysing lung cells through freeze-thawing virions are released and successfully infect BHK-21 cells. Following intranasal inoculation of BALB/cByJ mice with 10^4 PFU, lungs were collected at three different time points post-infection (5 dpi, 7 dpi and 10 dpi) and the viral replication of each virus was assessed by lung viral titration. After the incubation period viral plaques were counted using a magnifying glass and the PFU/lung was calculated (Fig.8).

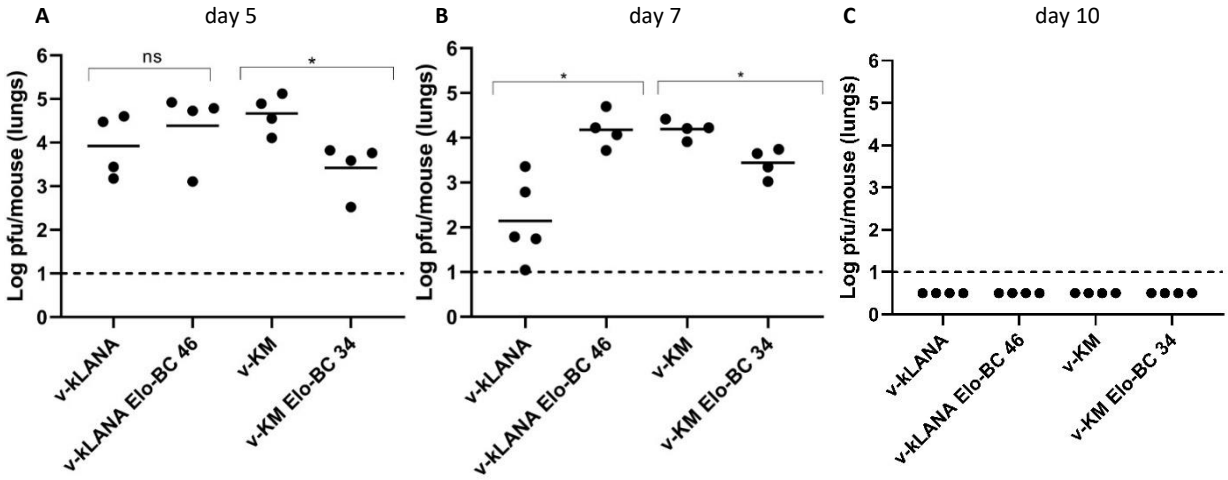

Figure 8- Lung viral titration. BALB/cByJ mice were intranasally inoculated with 10^4 PFU. Lung virus titers at days 5, 7 and 10 post-infection. Black circles represent individual mice. Horizontal bars indicate the means. The dashed line indicates the limit of detection. *, P < 0.05; ns, non-significant, Mann-Whitney test.

As shown in figure 8, all viruses undergo lytic replication in acutely infected lungs. Furthermore, both control viruses used in the experiment, v-kLANA and v-KM, showed a normal pattern of lytic infection, as already described (Miranda *et al.*, 2018). Levels of infection at day 5 post-infection were similar between all viruses (Fig.8 A), although a slightly lower titers were observed for the v-KM Elo-BC 34 in comparison to v-KM. At 10 days post-infection all viruses

were under the limit of infection detection, which indicates that the infection was cleared (Fig.8 C). This is known to coincide with the dissemination of virus through the lymphoid organs in order to establish and amplify latency in the spleen and lymph nodes. That there were no large alterations in lung lytic replication of the kLANA mutant virus is not unexpected, since mutations within the SOCS-box-like motif of mLANA did not seem to affect viral replication *in vivo* (Rodrigues *et al.*, 2009). v-KM Elo-BC 46 appears to have a lower lytic infection in the lungs, when compared to the control v-KM, which may suggest a further role of the BC-box present in the kLANA ORF. Finally, the apparent lower levels of lytic infection in v-kLANA infection group at 7 days post-infection (Fig.8 B), is likely due to some error during the inoculation or titration procedure, therefore the experiment would need to be repeated in order to confirm the infection values.

3.2 Infectious center assay and quantification of viral DNA-positive total splenocytes

A key feature of all herpesviruses infection is their lifelong persistence in the host by maintaining a viral latency program, which is carried out in more than 90% of infected cells and has led to the characterization of the latency-associated nuclear antigen (LANA) (Purushothaman *et al.*, 2016). Indeed, LANA is the main character of the viral latent phase and, among other functions, is able to modulate the ubiquitination pathway of its host through E3 ubiquitin-ligase activity (Cerqueira *et al.*, 2016). This role in the ubiquitination process is due to the bipartite SOCS-box motif divided into a Cullin-box and a BC-box located within LANA C-terminal and N-terminal regions, respectively. Thus, to assess the ability of the recombinant viruses, with the mutated BC-box, to establish latency in the spleens, BALB/cByJ mice were intranasally inoculated with 10^4 PFU of the respective virus (described in section 5.1 of Materials and Methods).

The infectious center assay is based on the latent virus ability to reactivate on permissive BHK-21, leading to the formation of viral plaques. Thus, following inoculation, mice were sacrificed at 3 different time points post infection (10 dpi, 14 dpi and 21 dpi) and their spleens were removed. Single cell suspensions were prepared and co-cultured with BHK-21 cells for 5 days. Co-culture with BHK-21 leads to viral reactivation from latency and formation of viral plaques in the BHK-21 monolayer. These viral plaques are counted which enables the calculation of a viral titer (or infectious center) per spleen (Fig.9 I, closed circles). In parallel, the splenocyte suspensions were freeze-thawed, to kill cells, and inoculated into BHK-21 cells to verify if any lytic infectious viruses (pre-formed viruses) were present in the splenocytes suspensions (Fig.9 I open circles).

To confirm the phenotype observed in the reactivation assay, a limiting dilution assay on total splenocytes was also performed (Fig.9 II). The frequency of viral DNA positive cells is highly relevant as it does not depend on the virus ability to reactivate *ex vivo*, representing an

independent method to assess viral latency. Viral DNA was detected by real-time PCR analysis using primers and probe sets specifically for the MHV68 M9 gene. Combining limiting dilution of

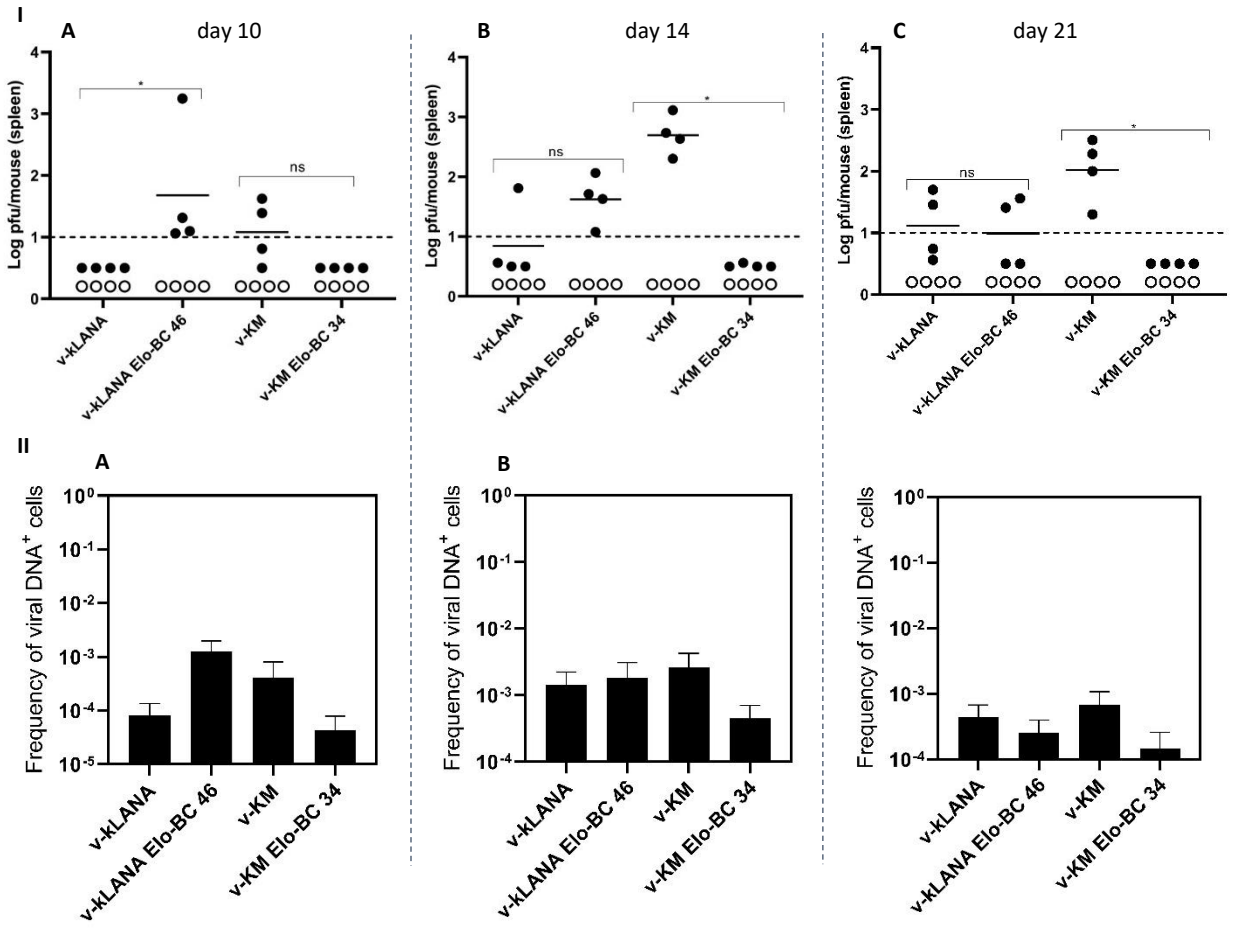

Figure 9 - **Assessment of latent infection in the spleens of infected mice.** BALB/cByJ mice were intranasally inoculated with 10^4 PFU. I) Infectious center/reactivating virus titers in spleens of infected. Black symbols, reactivating virus titers; open symbols, preformed infectious virus titers. Circles represent individual mice. Horizontal lines indicate the mean. The dashed line indicates the limit of detection. *, $P < 0.05$; ns, non-significant, Mann-Whitney test. II) Frequency of viral DNA^+ cells in total splenocytes. Data are from pools of 4 mice per group. Errors bars indicate 95% confidence intervals.

splenocytes with viral DNA detection, the frequency of latently infected splenocytes at 10, 14 and 21 days post-infection was calculated.

Graphic analysis from both experiments, infectious center assay (Fig.9 I) and limiting dilution assay (Fig.9 II) indicate that the results obtained are in accordance and there were no pre-formed viruses in the analyzed samples. Both control viruses, v-kLANA and v-KM, exhibited latency infection values according to the ones already described, with v-kLANA presenting lower levels of latency compared to v-KM (Habison *et al.*, 2017; Miranda *et al.*, 2018). At 10 days post-infection most mice did not present fully infected spleens. On the other hand, at day 14 post-infection, where latency is supposed to reach its peak in MHV68 infected mice, there was a high

number of viral DNA positive cells in almost every virus, except for the v-KM Elo-BC 34. Although the infectious center assay showed a slight difference between v-kLANA and v-kLANA Elo-BC 46 at 14 dpi, the limiting dilution assay clearly indicates that the number of viral DNA positive cells in both infectious groups is identical (Fig.9 II, B). Finally, at 21 days post-infection almost all viruses displayed a significantly low frequency of viral DNA positive cells which is in accordance with the infectious center assay.

Following the *in vitro* results demonstrated by (Cai *et al.*, 2006), v-kLANA Elo-BC 46 was expected to be unable to successfully establish latency in GC B cells. Instead, data generated in this project shows that v-kLANA Elo-BC 46 has identical latency infection values as the control v-kLANA. One possible explanation is that the remaining five amino acid residues of the BC-box are able to maintain box function and interact with the Cullin-box, assembling the EC_5S ubiquitin-ligase, thus modulating the host ubiquitination pathway and establishing persistent latent infection in the spleen.

A few years later, *in vivo* work developed by (Rodrigues *et al.*, 2009) at the mLANA SOCS-box-like motif, showed that functional deletion of this SOCS-box-like motif suppressed MHV68 expansion in GC B cells and prevented its persistent infection in mice. Thus, v-KM Elo-BC 34, a chimeric virus which encodes the BC-box at the N-terminal region plus the SOCS-box-like motif of mLANA at the C-terminal region (Fig.4), was thought to rescue the EC_5S ubiquitin-ligase activity and successfully establish latency through its SOCS-box-like motif of mLANA. However, the results showed the opposite, v-KM Elo-BC 34 has lower latency infection values when compared to the control v-KM. These results may suggest that, despite v-KM Elo-BC 34 having the mLANA SOCS-box-like motif, it may function as a Cullin-box, as they share some sequence homology (Fig.4), and still interact with the BC-box for the assembly of EC_5S ubiquitin-ligase complex, in an *in vivo* environment of infection.

Given this project results, the role and importance of kLANA's BC-box in the establishment of long persistent latent infection in the host remains unclear. Hence, further investigation needs to be done in order to characterize the BC-box and to confirm the phenotypes described in this project or to detect if some random mutation was introduced during the mutagenesis procedure. For that purpose, independent viral clones need to be analyzed, as well as the virus generated in the yfp background. Additionally, protein interactions between the BC-box and the Elongin BC and the SOCS-box-like with the Cullin 5 may be important in order to better understand the mechanisms underlying the EC_5S ubiquitin-ligase complex in the v-KM viruses.

Table 9 - Reciprocal frequency of viral DNA positive cells in total splenocytes

Cell population	D.p.i.	Virus	Reciprocal frequency[b] of viral DNA positive cells (95% CI)
Total splenocytes	10	v-Klana	12356.7 (7383.9-37841.5)
		v-pcr46	786.6 (507.1-1753.3)
		v-994	2453.9 (1237.8-139350.7)
		v-swap34	22867.1 (12664.6-117625.9)
	14	v-kLANA	693.2 (449.0-1519.9)
		v-pcr46	550.4 (323.8-1834.5)
		v-994	385.6 (235.7-1058.6)
		v-swap34	2200.2 (1433.5-4730.0)
	21	v-kLANA	2269.3 (1485.5-4804.3)
		v-pcr46	3975.5 (2528.2-9298.8)
		v-994	1470.3 (932.4-3474.9)
		v-swap34	6820.8 (3890.1-27657.0)

[a]Data were obtained from pools of four mice per group

[b]Frequencies were calculated by limiting dilution coupled to real-time PCR, with 95% confidence intervals (CI).

Chapter 5: Conclusion and future perspectives

KSHV persistent infection is highly associated with human malignancies, including some types of tumors (Dirk P. Dittmer, 2013). This virus is able to induce proliferation of latently infected B cells through reactions that occur in the germinal center, expanding latency and gaining access to memory B cells, the major reservoir of gammaherpesviruses latency (Cerqueira *et al.*, 2016). LANA, a protein coded by KSHV, is considered the viral protein responsible for viral persistence and the major gene of the latent viral lifecycle (Correia *et al.*, 2013; Purushothaman *et al.*, 2016). Previous works have shown that LANA protein has a bipartite SOCS-box motif divided into a Cullin-box and a BC-box located within its C-terminal and N-terminal regions, respectively (Cai *et al.*, 2006). Moreover, this BC-box interacts with an Elongin C and establishes a LANA-Elongin BC complex which is capable of assembling with a Cullin/Rbx1 module and reconstitute a complex protein with E3 ubiquitin-ligase activity (Cai *et al.*, 2006). This complex protein assembles an EC_5S

ubiquitin ligase, which enables the virus to hijack the E3 ligase components of the cell, thus modulating the ubiquitination pathway of its host (Cerqueira *et al.*, 2016).

In this project, by taking advantage of the MHV68 *in vivo* model to study KSHV pathogenesis, chimeric viruses with engineered mutations within the BC-box were generated in order to assess the importance of the BC-box motif within the kLANA N-terminal region.

Results showed that mutations within kLANA BC-box neither affect protein expression or viral growth *in vivo*, as both v-kLANA Elo-BC 46 and v-KM Elo-BC 34 viruses were able to replicate and wt-titers obtained. In vitro growth will need to be assessed in the future in more detail, in an *in vitro* growth curve. Viral lytic phase in the lungs was not significantly affected, although results need confirmation in future repeat experiments. Latency results were not conclusive and therefore the importance and role of kLANA BC-box is still unclear and viral phenotypes need to be reassessed. On the bright side, independent clones were already generated in this project, as well as the yfp versions of each chimeric mutant virus. Consequently, further studies to evaluate the viral phenotypes described in this project can be done in the immediate future. Indeed, these independent viruses will be crucial to assess if any phenotype observed is due to the introduced mutations, and not spurious mutations that could have occurred during generation of viruses. Another possible approach would be to mutate the whole BC-box, instead of just the first six amino acids, assuring complete loss of function.

Work developed here will facilitate future studies in order to describe and better understand the molecular mechanisms underlying kLANA SOCS-box motif. Such studies may include protein interactions between kLANA, Elongin C, Cullin 5, Rbx1 and tumor suppressors VHL or p53, which are thought to be degraded after ubiquitination with the crucial intervention of LANA (Cai *et al.*, 2006). Moreover, pharmacological targeting of viral E3 activity by screening potential E3-ubiquitin ligase inhibitors, despite challenging, may represent a great opportunity towards latency impairment.

References

Adler, H. *et al.* (2000) 'Cloning and Mutagenesis of the Murine Gammaherpesvirus 68 Genome as an Infectious Bacterial Artificial Chromosome', 74(15), pp. 6964–6974.

Adler, H. *et al.* (2001) 'Virus Reconstituted from Infectious Bacterial Artificial Chromosome (BAC) - Cloned Murine Gammaherpesvirus 68 Acquires Wild-Type Properties In Vivo Only after Excision of BAC Vector Sequences', 75(12), pp. 5692–5696. doi: 10.1128/JVI.75.12.5692.

Akula, S. M. *et al.* (2002) 'Integrin α3β1 (CD 49c/29) is a cellular receptor for Kaposi's sarcoma-associated herpesvirus (KSHV/HHV-8) entry into the target cells', *Cell*, 108(3), pp. 407–419. doi: 10.1016/S0092-8674(02)00628-1.

Aneja, K. K. and Yuan, Y. (2017) 'Reactivation and lytic replication of Kaposi's sarcoma-associated herpesvirus: An update', *Frontiers in Microbiology*, 8(APR), pp. 1–23. doi: 10.3389/fmicb.2017.00613.

Barbera, A. J. *et al.* (2006) 'The nucleosomal surface as a docking station for Kaposi's sarcoma herpesvirus LANA', *Science*, 311(5762), pp. 856–861. doi: 10.1126/science.1120541.

Di Bartolo, D. L. *et al.* (2008) 'KSHV LANA inhibits TGF-beta signaling through epigenetic silencing of the TGF-beta type II receptor.', *Blood*, 111(9), pp. 4731–4740. doi: 10.1182/blood-2007-09-110544.

Boshoff, C. and Chang, Y. (2001) 'Kaposi's sarcoma - Associated herpesvirus: A new DNA tumor virus', (2). Available at: http://discovery.ucl.ac.uk/1299672/.

Cai, Q. L. *et al.* (2006) 'EC5S ubiquitin complex is recruited by KSHV latent antigen LANA for degradation of the VHL and p53 tumor suppressors', *PLoS Pathogens*, 2(10), pp. 1002–1012. doi: 10.1371/journal.ppat.0020116.

Callis, J. (2014) 'The Ubiquitination Machinery of the Ubiquitin System', *The Arabidopsis Book*, 12, p. e0174. doi: 10.1199/tab.0174.

Cerqueira, S. A. *et al.* (2016) 'Latency-Associated Nuclear Antigen E3 Ubiquitin Ligase Activity Impacts Gammaherpesvirus-Driven Germinal Center B Cell', 90(17), pp. 7667–7683. doi: 10.1128/JVI.00813-16.Editor.

Chakraborty, S., Veettil, M. V. and Chandran, B. (2012) 'Kaposi's sarcoma associated herpesvirus entry into target cells', *Frontiers in Microbiology*, 3(JAN), pp. 1–13. doi: 10.3389/fmicb.2012.00006.

Chang, Y. *et al.* (1994) 'Identification of herpesvirus-like DNA sequences in AIDS-associated Kaposi's sarcoma', *Science (New York, N.Y.)*, 266(5192), pp. 1865–1869. doi: 10.1126/science.7997879.

Chudasama, P. *et al.* (2015) 'Structural proteins of Kaposi's sarcoma-associated herpesvirus antagonize p53-mediated apoptosis', *Oncogene*, 34(5), pp. 639–649. doi: 10.1038/onc.2013.595.

Cloutier, N. and Flamand, L. (2010) 'Kaposi sarcoma-associated herpesvirus latency-associated nuclear antigen inhibits interferon (IFN) β expression by competing with IFN regulatory factor-3 for binding to IFNB promoter', *Journal of Biological Chemistry*, 285(10), pp. 7208–7221. doi: 10.1074/jbc.M109.018838.

Collins, C. M. and Speck, S. H. (2012) 'Tracking murine gammaherpesvirus 68 infection of germinal center B cells in vivo', *PLoS ONE*, 7(3), pp. 1–11. doi: 10.1371/journal.pone.0033230.

Connor, M. O., Peifer, M. and Bender, W. (1989) 'Construction of large DNA segments in Escherichia

coli', *Science*.

Cooper, G. M. (1995) *Oncogenes*. second. Jones & Bartlett Learning.

Correia, B. *et al.* (2013) 'Crystal Structure of the Gamma-2 Herpesvirus LANA DNA Binding Domain Identifies Charged Surface Residues Which Impact Viral Latency', *PLoS Pathogens*, 9(10). doi: 10.1371/journal.ppat.1003673.

Dirk P. Dittmer, B. D. (2013) 'Kaposi sarcoma associated herpesvirus pathogenesis (KSHV) - an update', *Current Opinion in Virology*, pp. 1–12. doi: 10.1038/jid.2014.371.

Dissinger, N. J. and Damania, B. (2016) 'Recent advances in understanding Kaposi's sarcoma-associated herpesvirus', *F1000Research*, 5(0), p. 740. doi: 10.12688/f1000research.7612.1.

Dittmer, D. *et al.* (1999) 'Experimental transmission of Kaposi's sarcoma-associated herpesvirus (KSHV/HHV-8) to SCID-hu Thy/Liv mice.', *The Journal of experimental medicine*, 190(12), pp. 1857–1868.

Dittmer, D. P. *et al.* (2016) 'Kaposi sarcoma – associated herpesvirus : immunobiology , oncogenesis , and therapy Find the latest version : Kaposi sarcoma – associated herpesvirus : immunobiology , oncogenesis , and therapy', 126(9), pp. 3165–3175. doi: 10.1172/JCI84418.KSHV.

Dong, S., Forrest, J. C. and Liang, X. (2017) 'Murine gammaherpesvirus 68: A small animal model for gammaherpesvirus-associated diseases', *Advances in Experimental Medicine and Biology*, 1018, pp. 225–236. doi: 10.1007/978-981-10-5765-6_14.

Fujimuro, M. *et al.* (2003) 'A novel viral mechanism for dysregulation of β-catenin in Kaposi's sarcoma-associated herpesvirus latency', *Nature Medicine*, 9(3), pp. 300–306. doi: 10.1038/nm829.

Garber, A. C., Hu, J. and Renne, R. (2002) 'Latency-associated nuclear antigen (LANA) cooperatively binds to two sites within the terminal repeat, and both sites contribute to the ability of LANA to suppress transcription and to facilitate DNA replication', *Journal of Biological Chemistry*, 277(30), pp. 27401–27411. doi: 10.1074/jbc.M203489200.

Goossens, N. and Hoshida, Y. (2015) 'Hepatitis C virus-induced hepatocellular carcinoma', *Clinical and molecular hepatology*, 21(2), pp. 105–114. doi: 10.3350/cmh.2015.21.2.105.

Gramolelli, S. and Schulz, T. F. (2015) 'The role of Kaposi sarcoma-associated herpesvirus in the pathogenesis of Kaposi sarcoma', *Journal of Pathology*, 235(2), pp. 368–380. doi: 10.1002/path.4441.

Grinde, B. (2013) 'Herpesviruses: latency and reactivation - viral strategies and host response', *Journal of Oral Microbiology*. doi: 10.3402/jom.v5i0.22766.

Habison, A. C. *et al.* (2017) 'Cross-species conservation of episome maintenance provides a basis for in vivo investigation of Kaposi's sarcoma herpesvirus LANA', *PLoS Pathogens*, 13(9), pp. 1–25. doi: 10.1371/journal.ppat.1006555.

Heintz, N. (2001) 'Bac to the future: The use of bac transgenic mice for neuroscience research', *Nature Reviews Neuroscience*, 2(12), pp. 861–870. doi: 10.1038/35104049.

Hu, J. *et al.* (2014) 'LANA Binds to Multiple Active Viral and Cellular Promoters and Associates with the H3K4Methyltransferase hSET1 Complex', *PLoS Pathogens*, 10(7). doi: 10.1371/journal.ppat.1004240.

Inn, K.-S. *et al.* (2011) 'Inhibition of RIG-I-Mediated Signaling by Kaposi's Sarcoma-Associated Herpesvirus-Encoded Deubiquitinase ORF64', *Journal of Virology*, 85(20), pp. 10899–10904. doi:

10.1128/JVI.00690-11.

Jacobs, S. R. and Damania, B. (2011) 'The viral interferon regulatory factors of KSHV: Immunosuppressors or oncogenes', *Frontiers in Immunology*, 2(JUN), pp. 1–11. doi: 10.3389/fimmu.2011.00019.

Jacobs, S. R. and Damania, B. (2012) 'NLRs, inflammasomes, and viral infection', *Journal of Leukocyte Biology*, 92(3), pp. 469–477. doi: 10.1189/jlb.0312132.

Juillard, F. *et al.* (2016) 'Kaposi's sarcoma herpesvirus genome persistence', *Frontiers in Microbiology*, 7(AUG), pp. 1–15. doi: 10.3389/fmicb.2016.01149.

Krishnan, H. H. *et al.* (2004) 'Concurrent expression of latent and a limited number of lytic genes with immune modulation and antiapoptotic function by Kaposi's sarcoma-associated herpesvirus early during infection of primary endothelial and fibroblast cells and subsequent decline of l', *Journal of virology*, 78(7), pp. 3601–20. doi: 10.1128/JVI.78.7.3601.

Ma, Z. and Damania, B. (2016) 'The cGAS-STING Defense Pathway and Its Counteraction by Viruses', *Cell Host and Microbe*. Elsevier Ltd, 19(2), pp. 150–158. doi: 10.1016/j.chom.2016.01.010.

Marques, S. *et al.* (2003) 'Selective Gene Expression of Latent Murine Gammaherpesvirus 68 in B Lymphocytes Selective Gene Expression of Latent Murine Gammaherpesvirus 68 in B Lymphocytes', *Society*, 77(13), pp. 7308–7318. doi: 10.1128/JVI.77.13.7308.

Mesri, E. A., Cesarman, E. and Boshoff, C. (2010) 'Kaposi's sarcoma and its associated herpesvirus', *Nature Reviews Cancer*. Nature Publishing Group, 10(10), pp. 707–719. doi: 10.1038/nrc2888.

Miranda, M. P. De *et al.* (2018) 'In Vivo Persistence of Chimeric Virus after Substitution of the Kaposi ' s Sarcoma-Associated Herpesvirus LANA DNA Binding Domain with That of Murid Herpesvirus 4', *Journal of Virology*, pp. 1–13.

Moore, P. S. and Chang, Y. (2003) 'Kaposi's sarcoma-associated herpesvirus immunoevasion and tumorigenesis: two sides of the same coin?', *Annual review of microbiology*, 57, pp. 609–39. doi: 10.1146/annurev.micro.57.030502.090824.

Moore, P. S. and Chang, Y. (2010) 'Why do viruses cause cancer? Highlights of the first century of human tumour virology', *Nature Reviews Cancer*. Nature Publishing Group, 10(12), pp. 878–889. doi: 10.1038/nrc2961.

Okumura, F. *et al.* (2012) 'The role of Elongin BC-containing ubiquitin ligases', *Frontiers in Oncology*, 2(FEB), pp. 1–13. doi: 10.3389/fonc.2012.00010.

Parsons, C. H. *et al.* (2006) 'KSHV targets multiple leukocyte lineages during long-term productive infection in NOD/SCID mice', *Journal of Clinical Investigation*, 116(7), pp. 1963–1973. doi: 10.1172/JCI27249.

Pedro Simas, J. and Efstathiou, S. (1998) 'Murine gammaherpesvirus 68: A model for the study of gammaherpesvirus pathogenesis', *Trends in Microbiology*, 6(7), pp. 276–282. doi: 10.1016/S0966-842X(98)01306-7.

Prasad, A. *et al.* (2012) 'An Alternative Kaposi's Sarcoma-Associated Herpesvirus Replication Program Triggered by Host Cell Apoptosis', *Journal of Virology*, 86(8), pp. 4404–4419. doi: 10.1128/JVI.06617-11.

Purushothaman, P. *et al.* (2016) 'KSHV genome replication and maintenance', *Frontiers in Microbiology*,

7(FEB), pp. 1–14. doi: 10.3389/fmicb.2016.00054.

Rappocciolo, G. *et al.* (2006) 'DC-SIGN Is a Receptor for Human Herpesvirus 8 on Dendritic Cells and Macrophages', *The Journal of Immunology*, 176(3), pp. 1741–1749. doi: 10.4049/jimmunol.176.3.1741.

Rodrigues, L. *et al.* (2009) 'Termination of NF-κB activity through a gammaherpesvirus protein that assembles an EC"5S ubiquitin-ligase', *EMBO Journal*, 28(9), pp. 1283–1295. doi: 10.1038/emboj.2009.74.

Rodrigues, L. *et al.* (2013) 'Stabilization of Myc through Heterotypic Poly-Ubiquitination by mLANA Is Critical for γ-Herpesvirus Lymphoproliferation', *PLoS Pathogens*, 9(8). doi: 10.1371/journal.ppat.1003554.

Roizman B, Carmichael LE, Deinhardt F, de-The G, Nahmias AJ, Plowright W, Rapp F, Sheldrick P, Takahashi M, W. K. (1981) 'Herpesviridae. Definition, provisional nomenclature, and taxonomy.', *Intervirology*, pp. 16: 201-217.

Schulz, T. F. and Cesarman, E. (2015) 'Kaposi Sarcoma-associated Herpesvirus: Mechanisms of oncogenesis', *Current Opinion in Virology*. Elsevier B.V., 14, pp. 116–128. doi: 10.1016/j.coviro.2015.08.016.

Si, H. and Robertson, E. S. (2006) 'Kaposi's sarcoma-associated herpesvirus-encoded latency-associated nuclear antigen induces chromosomal instability through inhibition of p53 function.', *Journal of virology*, 80(2), pp. 697–709. doi: 10.1128/JVI.80.2.697-709.2006.

Stevenson, P. G. *et al.* (2002) 'K3-mediated evasion of CD8+ T cells aids amplification of a latent γ-herpesvirus', *Nature Immunology*, 3(8), pp. 733–740. doi: 10.1038/ni818.

Sun, R. *et al.* (1999) 'Kinetics of Kaposi ' s Sarcoma-Associated Herpesvirus Gene Expression Kinetics of Kaposi ' s Sarcoma-Associated Herpesvirus Gene Expression', 73(3), pp. 2232–2242.

Thakker, S. and Verma, S. C. (2016) 'Co-infections and pathogenesis of KSHV-associated malignancies', *Frontiers in Microbiology*, 7(FEB), pp. 1–14. doi: 10.3389/fmicb.2016.00151.

Toth, Z. *et al.* (2010) 'Epigenetic analysis of KSHV latent and lytic genomes', *PLoS Pathogens*, 6(7), pp. 1–17. doi: 10.1371/journal.ppat.1001013.

Virgin, H. W. th *et al.* (1997) 'Complete sequence and genomic analysis of murine gammaherpesvirus 68', *J Virol*, 71(8), pp. 5894–5904. Available at: http://jvi.asm.org/content/71/8/5894.full.pdf.

Wang, F. *et al.* (2003) 'Human Herpesvirus 8 Envelope Glycoprotein B Mediates Cell Adhesion via Its RGD Sequence', 77(5), pp. 3131–3147. doi: 10.1128/JVI.77.5.3131.

Wang, L.-X. *et al.* (2014) 'Humanized-BLT mouse model of Kaposi's sarcoma-associated herpesvirus infection', *Proceedings of the National Academy of Sciences*, 111(8), pp. 3146–3151. doi: 10.1073/pnas.1318175111.

Watanabe, T. *et al.* (2003) 'Kaposi's sarcoma-associated herpesvirus latency-associated nuclear antigen prolongs the life span of primary human umbilical vein endothelial cells.', *Journal of Virology*, 77(11), pp. 6188–96. doi: 10.1128/JVI.77.11.6188.

Wen, K. W. and Damania, B. (2010) 'Kaposi sarcoma-associated herpesvirus (KSHV): Molecular biology and oncogenesis', *Cancer Letters*. Elsevier Ireland Ltd, 289(2), pp. 140–150. doi: 10.1016/j.canlet.2009.07.004.

West, J. A. *et al.* (2011) 'Activation of Plasmacytoid Dendritic Cells by Kaposi's Sarcoma-Associated Herpesvirus', *Journal of Virology*, 85(2), pp. 895–904. doi: 10.1128/JVI.01007-10.

West, J. and Damania, B. (2008) 'Upregulation of the TLR3 Pathway by Kaposi's Sarcoma-Associated Herpesvirus during Primary Infection', *Journal of Virology*, 82(11), pp. 5440–5449. doi: 10.1128/JVI.02590-07.

Yoshimura, A., Naka, T. and Kubo, M. (2007) 'SOCS proteins, cytokine signalling and immune regulation', *Nature Reviews Immunology*, 7(6), pp. 454–465. doi: 10.1038/nri2093.

Supplementary data

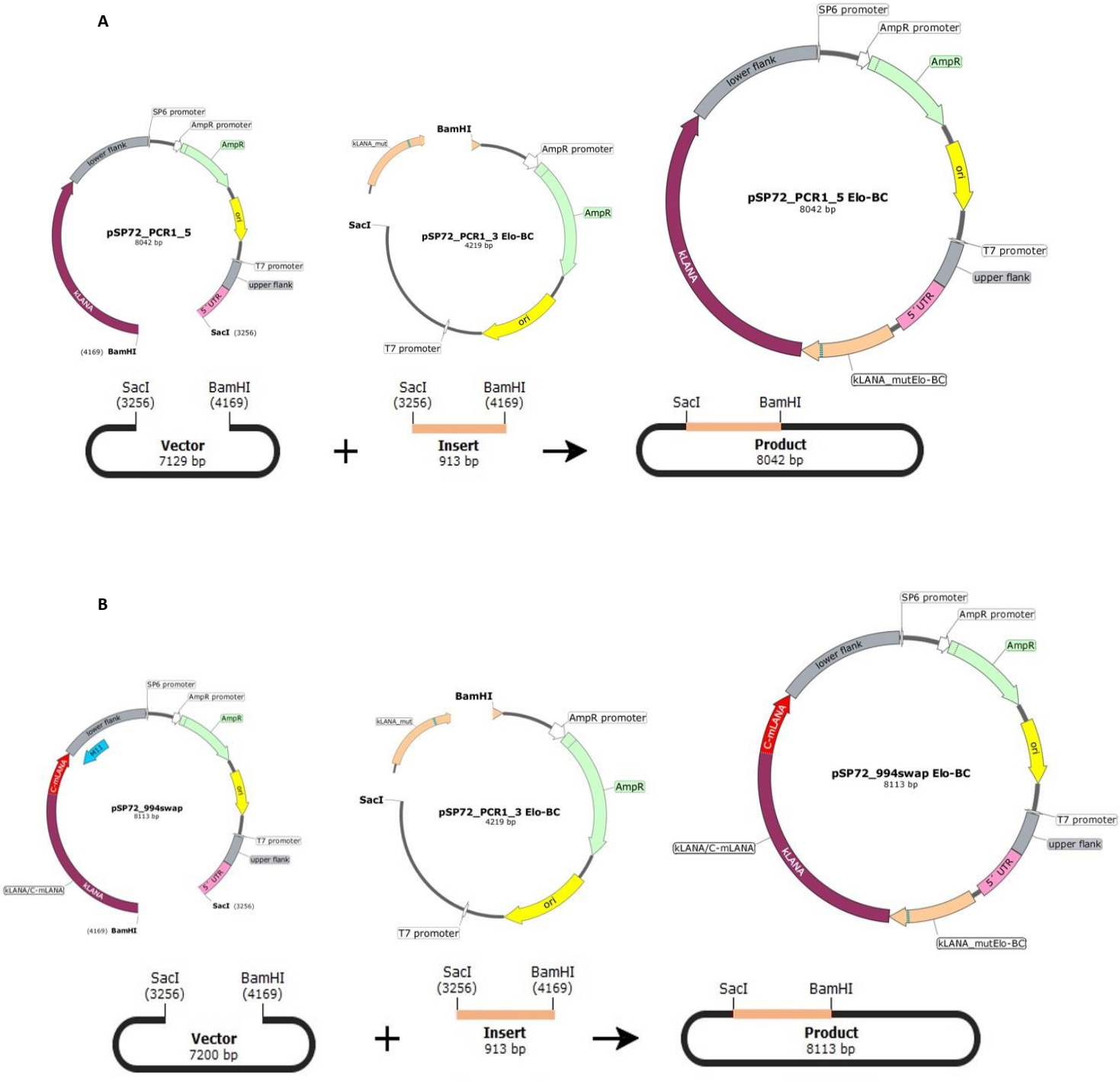

Figure 10 - Subcloning the pSP72_PCR1_3 Elo-BC into pSP72_PCR1_5 (A) and pSP72_994swap (B)

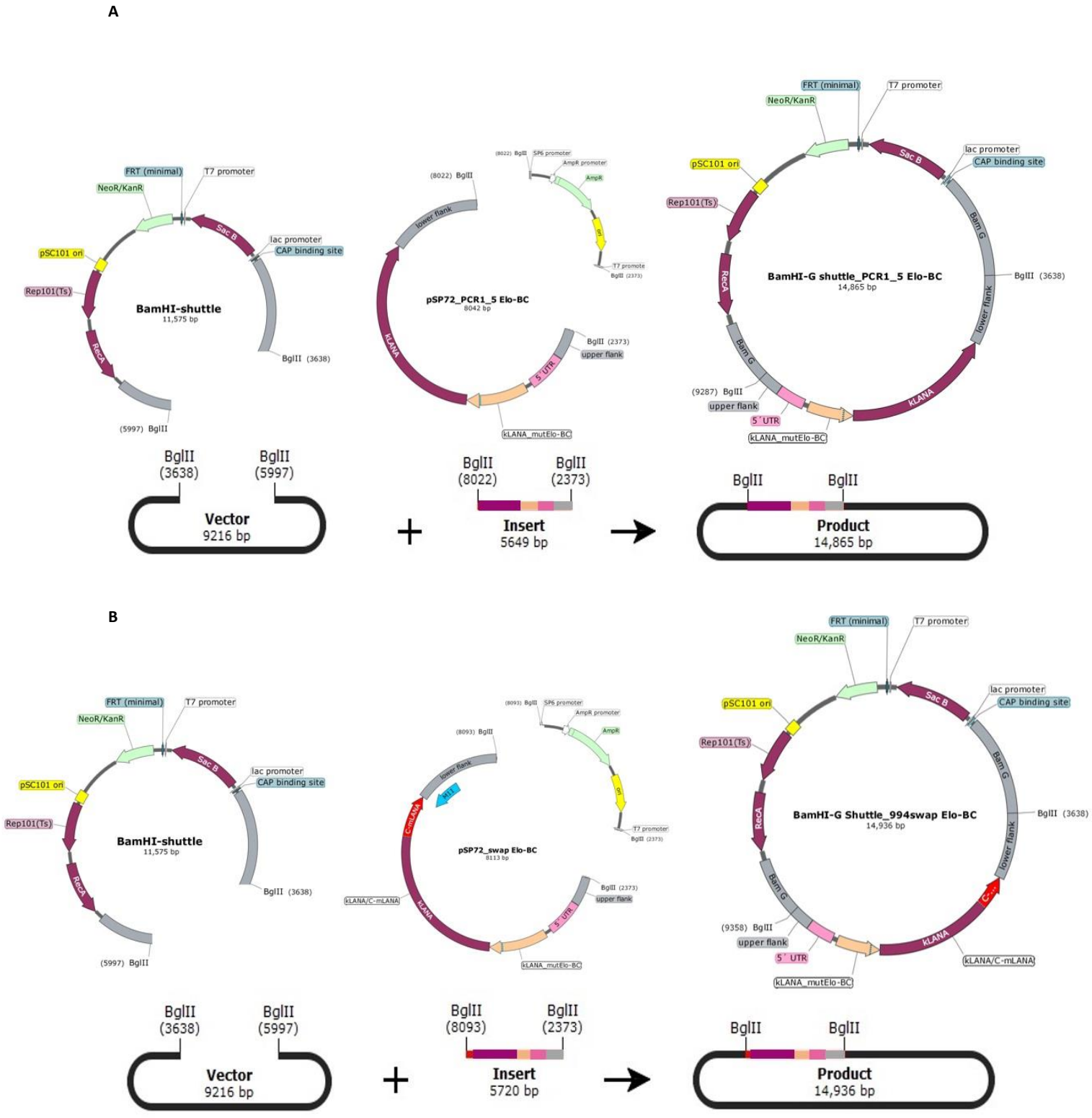

Figure 11 - Subcloning pSP72_PCR1_5 (A) and Elo-BC pSP72_swap Elo-BC (B) into BamHI-shuttle vector

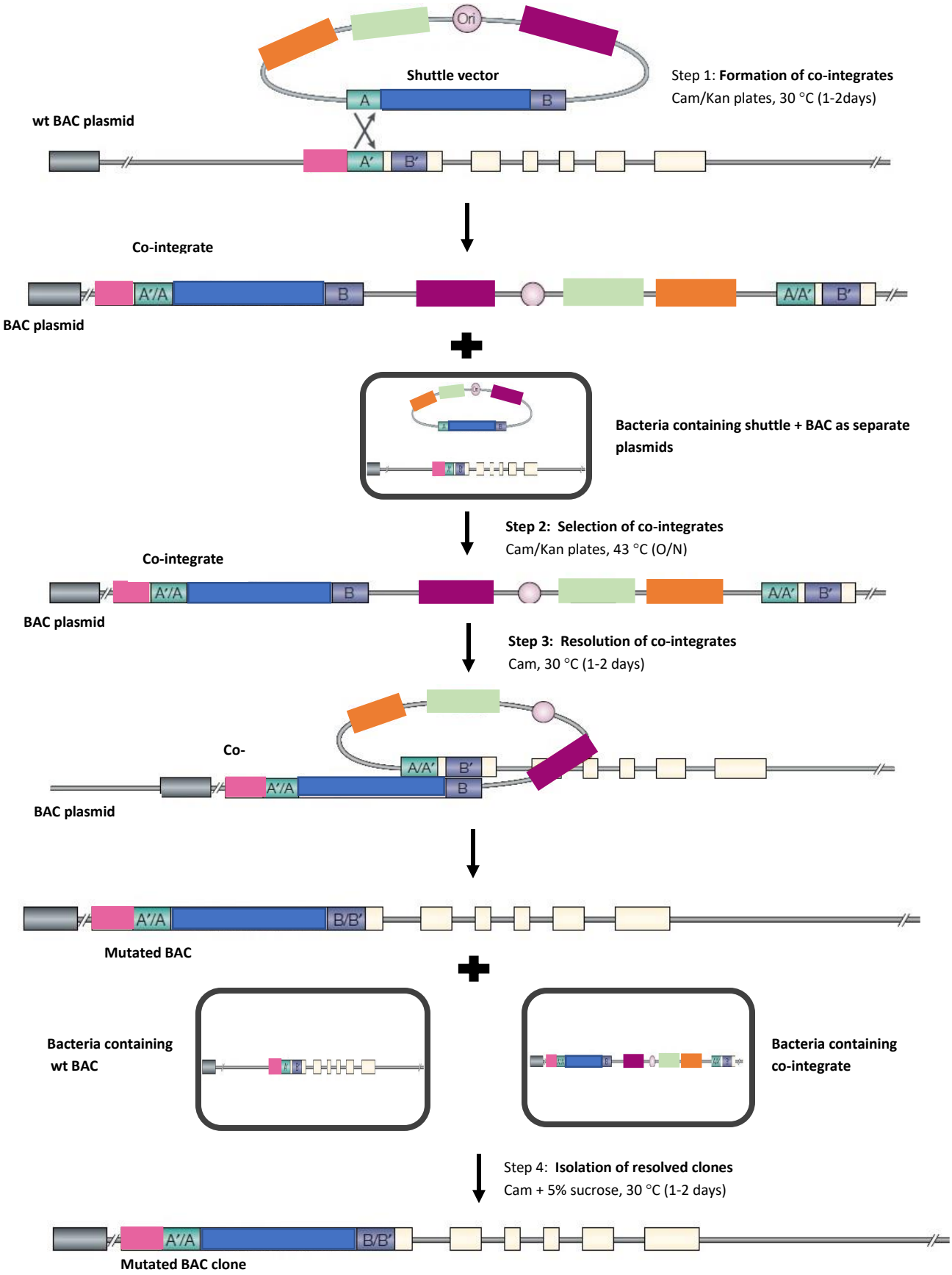

Figure 12 - BAC mutagenesis strategy. Boxes in orange represent the RecA gene, in purple the SacB gene, in gre**(Heintz, 2001)**n pink CamR and finally in blue the kLANA sequence, carrying the Elo-BC mutation. Adapted from (Heintz, 2001)

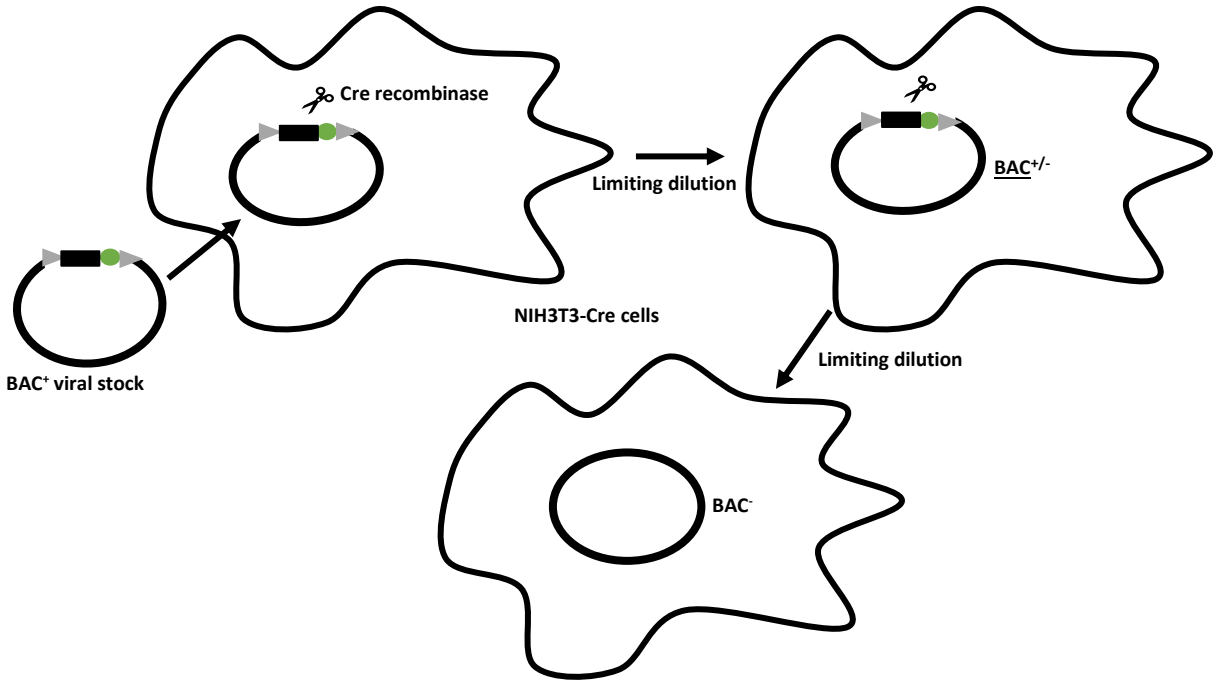

Figure 13- Passage through NIH3T3-Cre cells to remove BAC sequences. BAC cassette was removed by cell passage coupled with limiting dilutions. When the GFP signal was no longer observed, cells were scrapped, harvested and stored at -80 °C (BAC^- viral stocks)

BAC cassette

GFP

loxP sites